1   # An insight into neurotoxic and toxicity of spike fragments SARS-CoV-2 by

2   # exposure environment: A threat to aquatic health?

3

4

5   Ives Charlie-Silva[1]*, Amanda P. C. Araújo[2,3], Abraão T. B. Guimarães[2,3], Flávio P Veras[4], Helyson L.

6   B. Braz[5], Letícia G. de Pontes[6], Roberta J. B. Jorge[7]; Marco A. A. Belo[8,9], Bianca H V. Fernandes[10],

7   Rafael H. Nóbrega[11], Giovane Galdino[12], Antônio Condino-Neto[6], Jorge Galindo-Villegas[13], Glaucia

8   M. Machado-Santelli[14], Paulo R. S. Sanches[15], Rafael M. Rezende[16], Eduardo M. Cilli[15], Guilherme

9   Malafaia[2,3]*

10

11

12   [1]Department of Pharmacology, Institute of Biomedical Sciences, University of Sao Paulo (SP, Brazil).
13   [2]Post-graduation Program in Biotechnology and Biodiversity, Goiano Federal Institution and Federal
14   University of Goiás (GO, Brazil).
15   [3]Biological Research Laboratory, Post-graduation Program in Conservation of Cerrado Natural
16   Resources, Goiano Federal Institute – Urata Campus (GO, Brazil).
17   [4]Center of Research in Inflammatory Diseases, Ribeirão Preto Medical School,
18   University of São Paulo, Ribeirão Preto, São Paulo, Brazil.
19   [5]Postgraduate Program in Morphological Science, Department of Morphology, School of Medicine,
20   Federal University of Ceara, Delmiro de Farias St., 60.430-170, Fortaleza-CE, Brazil.
21   [6]Department of Immunology, Institute of Biomedical Sciences. University of Sao Paulo, Sao Paulo,
22   SP, Brazil (SP, Brazil).
23   [7]Drug Research and Development Center, Federal University of Ceara, Coronel Nunes de Melo St.,
24   1000, 60.430-275, Fortaleza-CE, Brazil; Department of Physiology and Pharmacology, School of
25   Medicine, Federal University of Ceara, Coronel Nunes de Melo St., 1127, 60.430-275, Fortaleza-
26   CE, Brazil.
27   [8]Laboratory of Animal Pharmacology and Toxicology, Brazil University, Descalvado, SP, Brazil.
28   [9]Department of Preventive Veterinary Medicine, São Paulo State University (UNESP),
29   Jaboticabal,SP, Brazil.
30   [10]Laboratório de Controle Genético e Sanitário, Diretoria Técnica de Apoio ao Ensino e
31   Pesquisa, Faculdade de Medicina da Universidade de São Paulo.
32   [11]Reproductive and Molecular Biology Group, Institute of Biosciences, São Paulo State University,
33   Botucatu, São Paulo, Brazil.
34   [12] Institute of Motricity Sciences, Federal University of Alfenas, Alfenas, MG, Brazil.
35   [13]Faculty of Biosciences and Aquaculture, Nord University, 8049 Bodø, Norway
36   [14]Department of Cell Biology, Institute of Biomedical Sciences, University of São Paulo, São Paulo,
37   Brazil.
38   [15]Institute of Chemistry, São Paulo State University (UNESP), Araraquara-SP, Brazil.
39   [16]Brigham and Women's Hospital, Harvard Medical School, 75 Francis St, Boston, United States.

40

41

42

43

44

45

46   ***Corresponding author:**

47   ***Ives Charlie-Silva PhD.**   e-mail: charliesilva4@hotmail.com

48   Department of Pharmacology, Institute of Biomedical Sciences, University of Sao Paulo (SP, Brazil)

49

50   ***Guilherme Malafaia. PhD.** e-mail: guilhermeifgoiano@gmail.com

51   Biological Research Laboratory, Goiano Federal Institution – Urata Campus, Rodovia Geraldo Silva

52   Nascimento, 2,5 km, Zona Rural, Urutaí, Brazil.

53

54

55

56

57

58

59   **HIGHLIGHTS**

60

61   • SARS-CoV-2 spike protein peptides (PSDP) were synthesized, purified, and characterized by
62   solid phase peptide synthesis.

63   • PSDP peptides promoted REDOX imbalance and acute neurotoxicity in tadpoles
64   (*Physalaemus cuvieri*)

65   • *In silico studies* have shown interactionsbetween peptides and acetylcholinesterase and
66   antioxidant enzymes

67   • Aquatic particle contamination of SARS-CoV-2 can constitute additional environmental
68   damage

69

70

ABSTRACT

The Spike protein (S protein) is a critical component in the infection of the new coronavirus (SARS-CoV-2). The objective of this work was to evaluate whether peptides from S protein could cause negative impact in the aquatic animals. The aquatic toxicity of SARS-CoV-2 spike protein peptides derivatives has been evaluated in tadpoles (n = 50 tadpoles / 5 replicates of 10 animals) from species *Physalaemus cuvieri* (Leptodactylidae). After synthesis, purification, and characterization of peptides (PSDP2001, PSDP2002, PSDP2003) an aquatic contamination has been simulatedwith these peptides during 24 hours of exposure in two concentrations (100 and 500 ng/mL). The control group ("C") was composed of tadpoles kept in polyethylene containers containing de-chlorinated water. Oxidative stress, antioxidant biomarkers and neurotoxicity activity were assessed. In both concentrations, PSPD2002 and PSPD2003 increased catalase and superoxide dismutase antioxidants enzymes activities, as well as oxidative stress (nitrite levels, hydrogen peroxide and reactive oxygen species). All three peptides also increased acetylcholinesterase activity in the highest concentration. These peptides showed molecular interactions in silico with acetylcholinesterase and antioxidant enzymes. Aquatic particle contamination of SARS-CoV-2 has neurotoxics effects in *P. cuvieri* tadpoles. These findings indicate that the COVID-19 can constitute environmental impact or biological damage potential.

88

89

Key words: oxidative stress; coronavirus; amphibians; acetylcholinesterase, SARS-Cov-2

GRAPHICAL ABSTRACT
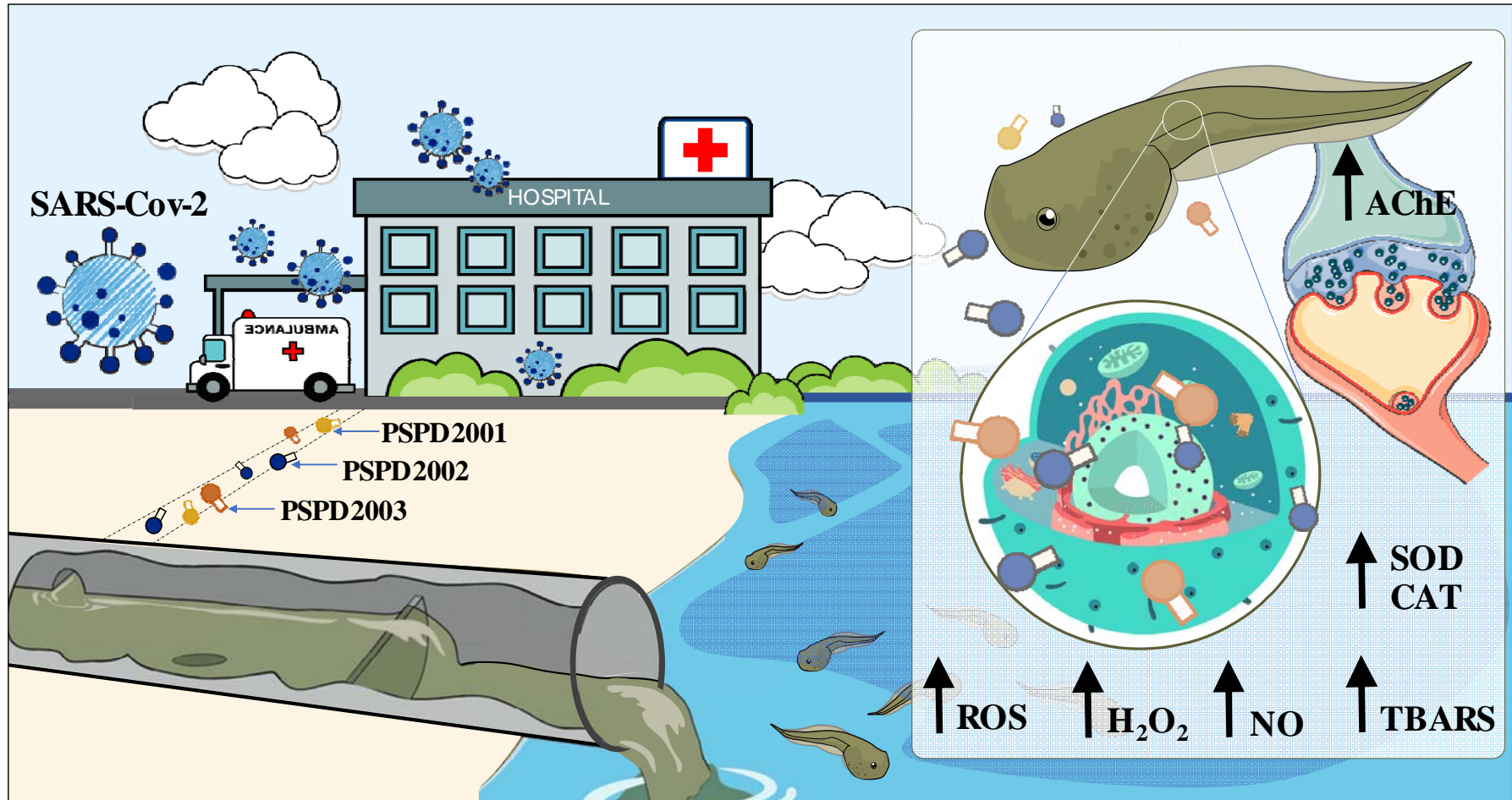
93   **1. INTRODUCTION**

94   Coronavirus Disease-2019 (COVID-19) pandemic, caused by SARS-CoV-2 (Severe acute
95   respiratory syndrome coronavirus 2), an emergent beta-coronavirus threatening human
96   health, has led to a dramatic worldwide crisis and presents unprecedented global challenges
97   on everybody's daily life, social aspects, political affairs, and health measures (Chakraborty &
98   Prasenjit, 2020)

99   Remarkably, the poor and the most vulnerable people are at critical high risk, and
100 Oxfam, an international confederation of 20 NGO's already calculates that nearly 500 million
101 people worldwide may succumb to poverty resulting from the same (OI, 2020). By Dec. 27,
102 over 79.2 million cases and over 1.7 million deaths have been reported since the start of the
103 pandemic (FAO, 2020). Resulting from the same, in only 12 months, we have learned a lot
104 about SARS-CoV-2. Our ability to test for and manage COVID-19 has improved, but ongoing
105 debate remains about how SARS-CoV-2 is transmitted (Editorial Lancet, 2020).

106   The most recurrent forms of SARS-CoV-2 transmission are through direct contact with
107 an infected person (Meyerowitz et al., 2020), inhaling respiratory droplets containing the
108 virus (Harrison et al., 2020), or accessing a contaminated environment where suspended
109 particles are present over longer distances and time than droplet transmission (Graham et al.
110 2020).

111   However, by reviewing the environmental threats of the virus reported so far, it is
112 concluded that the virus can survive on inanimate surfaces such as metal, glass, or plastic for
113 up to 9 days if any effective disinfection procedure with ozone, ethanol, hydrogen peroxide,
114 UV light, chlorine or its derivatives as sodium hypochlorite is not conducted in between
115 (Kampf et al. 2020).

116   Although the direct contact described above concerns meaningful, a different
117 environmental transmission source with the virus now recognized is the indirect contact
118 through the infected people's stool and urine (Chen et al., 2020; Xiao et al., 2020; Jones et al.,
119 2020). Unconventional studies support this notion by reporting positive SARS-CoV-2 viral
120 titers in domestic sewages (Pandey et al., 2020; Elsamadony et al., 2020; Polo et al., 2020).

121 So far, Sars-Cov-2 has been detected in several countries wastewaters of the American,
122 European, and Asian continents, suggesting as mandatory the monitoring of the secondary
123 transmission of the new coronavirus via wastewater (Liu et al. 2020). On a more compelling
124 perspective, strong evidence suggests that surveillance of primarily settled solids in
125 wastewater through one-step ddPCR is a solid strategy to track the spread of Covid-19 disease
126 transmission before the clinical cases break out in a particular location (Graham, 2020).

127 Moreover, following this trend can shed light on the characteristics of infection that are
128 difficult to capture in clinical investigations, such as the dynamics of infection and early viral
129 elimination (Wu et al., 2020).

130   The increase in the generation of household waste (Sharma et al., 2020; Zand& Heir,
131 2020; Urban et al., 2021), hospitals (Abu-Qdais et al., 2020; Sangkham, 2020; Yang et al.,
132 2020), and notable civil buildings (Carvalho et al., 2020; Abu-Rayash et al., 2020; Santiago et
133 al., 2020) constitute some of the environmental grounds where no information on the
134 ecotoxicological effects of SARS-CoV-2 proteic or genetic structural components impact on
135 freshwater vertebrates exists.

136   Therefore, this lack of knowledge requires urgent attention by developing studies to
137 assess how COVID-19 impacts the aquatic populations in the close vicinity of the
138 anthropogenic activities described above. Such studies may focus on supporting actions or
139 strategies on the remediation or at least mitigation of impacts in favor of conserving non-
140 target species at the edge of any Sars-Cov-2 variant.

141   The Spike (S) protein is a critical component of the new Sars-Cov-2 coronavirus found
142 on the surface of the SARS-Cov-2 virus, giving it a "crown" appearance. The S protein is a
143 granule-shaped structural protein with a length of about 1200 aa, which helps the virus bind
144 to cell receptors and mediates viral infection and pathogenesis (Coughlan, 2020). The S
145 protein plays a key role in the receptor recognition and cell membrane fusion process with
146 ACE-2 (angiotensin-converting enzyme 2) (Huang et al., 2020). Therefore, it is not surprising
147 this ligand-receptor interaction of the S protein is the primary target to produce vaccines
148 against COVID-19, as reported in different studies (Bangaru et al., 2020; Samrat et al., 2020;
149 Keech et al., 2020; Yang et al., 2020; Qi et al., 2020; Ravichandran et al., 2020).

150   Several in vivo platforms to dissect the cellular and molecular programs governing
151 Sars-Cov-2 viral dissemination on vertebrates are available. However, the number of aquatic
152 model animals that may support trials and provide reliable information is almost inexistent.
153 Among them, the zebrafish model represents an attractive model to explore the desired
154 effects on the context of a full vertebrate (Galindo-Villega, 2020). Unfortunately, the zebrafish
155 has not been vigorously infected in vivo trials so far by the causative agent of Covid-19
156 (Gaudin & Goetz, 2021).

157   Following a synthetic approach in previous research, we have developed three
158 peptides of the full-length SARS-CoV-2 Spike protein (PSPD2001, PSPD2002, and PSPD 2003)
159 after a pattern memorization phagolysosomal proteolysis (Fernandes et al. 2020). To attempt
160 to elucidate whether and how the Sars-Cov-2 influence the aquatic animals, in this study, we

161   investigate the same by adding the three produced synthetic peptides to mimic the resulting

162   Covid-19 aquatic contamination in wastewater. The tadpole *Physalaemus cuvieri*, is a prevalent

163   amphibian species found in many freshwater habitats throughout Brazil and South America

164   ((Miranda et al., 2019; Herek et al., 2020; Araújo et al., 2020ab; Rutkoski et al., 2020). Its

165   population stability and abundance in the areas that occur (Frost 2017), good adaptability in the

166   laboratory, and early biological response justify the species' choice (Herek et al., 2020; Araújo et

167   al., 2020ab; Rutkoski et al., 2020). Previous studies using this species report the effects of water

168   pollution caused by wastewater runoff (Wrubleswski et al. 2018). Therefore, in this study, we

169   selected *P. cuvieri* as our choice of a translational model vertebrate.

170   From different biomarkers indicative of an imbalance in oxidation-reduction (REDOX)

171   and neurotoxicity processes, we aimed to test the hypothesis that nanometric concentrations

172   of the SARS-CoV-2 Spike protein fragments in water may affect the health of amphibians. We

173   believe that studies like ours are needed not only to expand our knowledge about the impacts

174   of COVID-19 on aquatic biodiversity; but also to predict the environmental impacts of the

175   recent pandemic on the populations of neotropical amphibians, which have already, over the

176   years, shown a drastic population decline (Pechmann et al., 1991; Blaustein et al., 2002;

177   Ranvestel et al., 2004; Grant et al., 2020).

178

179

180   **2. MATERIAL AND METHODS**

181   **2.1. Synthesis, purification, and characterization of peptides**

182   **2.1.1. Synthesis of SARS-CoV-2 Spike protein peptides**

183   The peptides were obtained manually using the solid phase peptide synthesis method (SPFS)

184   using the Fmoc strategy (Raibaut et al., 2014; Behrendt et al., 2016). The couplings were carried

185   out by activating the carboxyl groups of the Fmoc-amino acids with a solution of

186   diisopropylcarbodimide and hydroxybenzotriazole (HOBT), for2 h. In this step, a 2-fold excess of

187   Fmoc-amino acids and coupling agents in relation to the number of reactive sites in the resin was

188   used. Deprotection of the amino group after coupling, i.e., removal of the base labile Fmoc group

189   was carried out by reaction with a 20% solution of 4-methyl-piperidine in dimethylformamide

190   (DMF) following the exit of the protective group through the colorimetric test ninhydrin (Luna et

191   al., 2016), which identifies free amine groups converting the yellow solution to violet-blue after

192   incubation at $110^{\circ}C$ for 3 min. The resins used for synthesis were Fmoc-Cys (Trt)-Wang, Fmoc-Thr

193   (TBu)-Wang, and Fmoc-Asn (Trt)-Wang for peptides Arg-Val-Tyr-Ser-Ser-Ala-Asn-Asn-Cys-

194 COOH (PSPD2001); Gln-Cys-Val-Asn-Leu-Thr-Thr-Arg-Thr-COOH (PSPD2002) and Asn-Asn-

195 Ala-Thr-Asn-COOH (PSPD2003), respectively

196 **2.1.2. Cleavage of SARS-CoV-2 Spike protein peptides**

197 After coupling all the amino acid residues from the peptide sequences, the chains were

198 removed from the solid support by acid cleavage using trifluoroacetic acid (TFA) for 2 h [similarly

199 to Guy & Fields (1997)]. In addition to TFA, reaction suppressors were added according to the

200 sequence of each peptide. After cleavage, the peptides were precipitated with cold ether and later

201 extracted with 0.045% TFA solution in purified water. The solutions were lyophilized to obtain solid

202 crude material.

203

204 **2.1.3. Purification of SARS-CoV-2 Spike protein peptides**

205 The crude compounds were purified by high-performance liquid chromatography (HPLC)

206 with a reverse-phase column using different purification methods according to the retention time

207 obtained in a gradient program of 5 to 95% in 30 min (exploration gradient) in Analytical HPLC

208 (Klaassen et al.,2019). Table S1 (see "Supplementary Material") presents a summary of the

209 purification methods adopted in our study. The purification solvents were water containing 0.045%

210 TFA (solvent A) and acetonitrile containing 0.036% TFA (solvent B).

211 After collecting, lyophilizing, and weighing the pure material fractions, its yield was

212 calculated, obtaining 13.0% for PSPD2001, 21.4% for PSPD2002, and 18.2% for PSPD2003. The

213 pure and solid material was subjected to chromatographic analysis to determine the purity of the

214 final product. Only compounds with purity equal to or greater than 95% were considered for

215 biological analysis,

216

217 **2.1.4. Characterization of SARS-CoV-2 Spike protein peptides**

218 The analysis of the synthesized peptides' identity was carried out in a mass spectrometer

219 (Metzgeret al., 1994)Thermo LCQ-fleet, with ESI-IT-MS configuration. For this, the sample

220 solutions were directly infused at a concentration of approximately 10 mg/L in acetonitrile/water

221 containing 0.1% v/v formic acid. The infusion rate was adjusted to 5.0 μL/min, and the electrospray

222 source was operated in a positive mode, applying 4.5 kV to the electrospray capillary.

223

224 **2.2. Alignment of SARS-CoV-2 Spike protein peptides**

225 The similarities between the PSPD2001, PSPD2002 and PSPD2003 peptides synthesized in

226 the present study were tested using the CLUSTAL W version 1.83 software [Higgins et al. (1996),

227 Pais et al. (2014) - http://www.ebi.ac.uk/clustalw/]. The peptides were aligned with proteins

228   deposited in the NCBI/BLAST (Basic Local Alignment Search Tool), consisting of a set of programs

229   that look for similarities between different sequences. The investigated sequences' alignment was

230   carried out with the nucleic acid and/or protein database (http://www.ncbi.nlm.nih.gov/blast).

231   Within BLAST, the search was carried out in the "Protein blast" using as a database the "Swissprot

232   protein sequence (swissprot)", algorithm - blastp (protein BLAST) and the search was restricted to

233   *Physalaemus cuvieri* (taxid:218685). The database UniProtKBSwissProt (http://www.uniprot.org/)

234   was used to obtain detailed information on the protein aligning with the selected peptides revealed.

235

236   **2.3. Model system and experimental design**

237   To evaluate the synthesized peptides' aquatic toxicity, we used tadpoles of the species

238   *Physalaemus cuvieri* (Leptodactylidae) as a model system. All tadpoles used came from an ovigerous

239   mass (containing approximately 1500 eggs), according to Pupin et al. (2010). They were collected in

240   a lentic environment (Urutaí, GO, Brazil) surrounded by native vegetation from the Cerrado biome,

241   under license no. 73339-1 of the Biodiversity Authorization and Information System

242   (SISBIO/MMA/ICMBio) in Brazil.

243   Upon arrival at the laboratory, the eggs were kept in an aquarium (40.1 x 45.3 x 63.5 cm)

244   containing 80 L of naturally dechlorinated water (for at least 24 h), under controlled light

245   conditions (light-dark cycle, 12:12 h), temperature (26 °C ± 1 °C - similar to the natural

246   environment) and constant aeration (maintained by air compressors), being fed once a day (ad

247   libitum) with commercial fish food (guarantee levels: 45% crude protein, 14% ether extract, 5%

248   crude fiber, 14% mineral matter and 87% dry matter). After the eggs hatched, the tadpoles

249   remained in these conditions until they reached stage 27G, according to Gosner (1960) (body

250   biomass: 70 mg ± 4.1 mg and total length: 20.1 mm ± 0.7 mm - mean ± SEM). The healthy

251   tadpoles (i.e., with normal swimming movements and without morphological deformities or

252   apparent lesions) were divided into seven experimental groups (n = 50 tadpoles / each - 5 replicates

253   composed of 10 animals/each. The control group ("C") was composed of tadpoles kept in

254   polyethylene containers containing 50 ml of de-chlorinated water, free of any peptide. The animals

255   kept in water containing the peptides comprised the groups "PSPD2001", "PSPD2002", and

256   "PSPD2003". Two concentrations were tested for each peptide (100 and 500 ng/mL, defined based

257   on reports that SARS-CoV-2 in sweet environments occurs in minimal concentrations (Shutler et

258   al., 2020; Guerrero-Latorre et al., 2020; Tran et al., 2020). The exposure period (24 h; in the static

259   system) was defined considering the low persistence of SARS-CoV-2 in the aquatic environment

260   after being released with human feces (Bivins et al., 2020).We emphasize that, throughout the

261   exposure period, different physical-chemical parameters of the quality of the exposure waters were

262   monitored (every 6 hours), keeping them equitable between treatments (temperature: 23ºC ± 1.14;

263   atmospheric pressure (atm) : 0.91 ± 0.0001; electrical resistivity (Ωm): 0.01 ± 0.0001; electrical

264   conductivity (μS/cm^2): 96.2 ± 1.83; total dissolved solids (mg/L): 48, 2 ± 0.83; salinity: 0.04 ±

265   0.004; oxidation-reduction potential (ORP): 130.21 ± 6.17; dissolved oxygen (mg/L): 7.72 ± 0.78

266   and pH: 7 , 2 ± 0.38).

267

268   **2.4. Toxicity biomarkers**

269   We evaluated peptide-induced toxicity from predictive biomarkers of REDOX imbalance

270   and neurotoxicity after exposure, considered classic and essential parameters in ecotoxicological

271   studies (Valavanidis et al., 2016). For this, pools of four animals/each composed the samples to be

272   analyzed. Such animals were weighed and later macerated in 1 mL of phosphate-buffered saline

273   (PBS), centrifuged at 13.000 rpm for 5 min (at 4ºC). Thesupernatant was separated into aliquots to

274   be used in different biochemical evaluations. Entire bodies were used in the experiment due to the

275   hard time isolating specific organs from small animals. Organ-specific biochemical assessment in

276   tadpole requires highly accurate dissection due to their small size, making it difficult to process large

277   sample numbers under a time constraint (Khan et al. 2015). Organ "contamination" by organic

278   matter and/or by other particles consumed by tadpole can be biased at biochemical analysis applied

279   to organs at dissection time (Lusher et al. 2017; Guimarães et al., 2021).

280

281   **2.4.1. REDOX state**

282   **2.4.1.1. Oxidative stress biomarkers**

283   The effects of exposure to peptides on oxidative stress reactions were evaluated based on

284   indirect nitric oxide (NO) determination on REDOX regulated processes via nitrite measurement

285   (Soneja et al. 2005); thiobarbituric acid reactive species (TBARS), a predictive of lipid peroxidation

286   (De-Leon & Borges, 2020); production of reactive oxygen species (ROS) and on hydrogen peroxide

287   (H_2O_2), which plays an essential role in responses to oxidative stress in different cell types (Sies,

288   2017). The Griess colorimetric reaction was used to measure NO (Grisham et al., 1996). This

289   reaction consisted of detecting nitrite resulting from NO oxidation. TBARS levels were determined

290   based on procedures described by Ohkawaet al. (1979) and modified by Sachettet al. (2020), with

291   adaptations for conduction in microtubes and ELISA microplate reading. The reagent of 1.1,3.3-

292   tetra-ethoxy-propane was used as a standard solution in the reaction with thiobarbituric acid (TBA)

293   reactive substance, according Ro et al. (2020). In brief, this method's principle depends on the

294   Determination of the pink color produced by TBA interaction with malondialdehyde (MDA). The

295   production of hydrogen peroxide and ROS was evaluated using the methodologies proposed by

296   Elnemma et al. (2004) and Maharajan et al. (2018).

297

298

299

300   2.4.1.2. Antioxidant response biomarkers

301   The activation or suppression of antioxidant activity by peptides was assessed by determining

302   catalase and superoxide dismutase (SOD) enzyme activities, which are considered critical first-line

303   antioxidants for defense strategies against oxidative stress (Ighodaro&Akinloye, 2018; Jing et al.,

304   2020). While catalase activity was assessed based on Sinha et al. (1972) andMontalvão et al.

305   (2021). The SOD was determined according to the method described by Del-Maestro & McDonald

306   (1985) (initially) and adapted by Estrela et al. (2021). To assess the balance between the synthesis

307   of hydrogen peroxide by SOD and its decomposition by catalase, the SOD/CAT ratio was calculated

308   and recorded, as Liu et al. (2017).

309

310   2.4.2. Neurotoxicity

311   Peptide neurotoxicity was assessed by quantifying acetylcholinesterase (AChE) activity,

312   based on the method by Ellman et al. (1961), with minor detailed modifications in Estrela et al.

313   (2021). AChE activity is used as a cholinergic function marker since it regulates the acetylcholine

314   (ACh) amount interacting with its receptors (Tougu, 2001).

315

316   2.4.3. Determination of the protein level

317   All results of the biochemical analyzes were expressed by the "g of proteins" of the samples.

318   In this case, the protein level was determined with a commercial kit (Bioténica Ind. Com. LTD,

319   Varginha, MG, Brasil. CAS number: 10.009.00) based on biuret reaction (Gornall et al., 1949;

320   Henry et al., 1957). In general, Cu^{2+} ions, in an alkaline medium, react with the peptide bonds of

321   proteins forming the blue complex specifically with protein, and the intensity of color, measured by

322   an ELISA reader at a wavelength of 492 nm, is proportional to the protein concentration.

323

324   2.5. Bioinformatics *in silico* analysis

325   Seeking to predict the binding mode and affinity of the bonds between the peptides

326   synthesized in our study and the protein structures of the enzymes AChE, catalase, and SOD, we

327   performed docking and chemoinformatic screens (Kolb et al., 2009). For this, we obtained the

328   peptide ligand PSPD2002 and PSPD2003 in three dimensions through the web server PEP-FOLD3

329 (https://bioserv.rpbs.univ-paris-diderot.fr/services/PEP-FOLD3/). Protein structures and sequences

330 of the *P.cuvieri* (i.e.:Leptodactylidae) taxonomic family were not found in the biological structure

331 databases. Therefore, we use as target structures those from the Xenopodinae family, a family

332 phylogenetically close to the group of Leptodactylidae (Jetz& Pyron, 2018). The AChE and catalase

333 enzymes' structures were obtained using the homology construction technique with values of

334 similarity 65.48% and 87.14% to structures (targets) used for comparative modeling on the server

335 SWISS-MODEL (https://swissmodel.expasy.org/), respectively. On the other hand, the structure of

336 the SOD was obtained by Research Collaboratory for Structural Bioinformatics protein databank

337 (https://www.rcsb.org) PDB code: 1XSO with 1.49Å resolution, obtained by X-ray diffraction of

338 Xenopodinae origin. For molecular docking simulations, AutoDock tools (ADT) v4.2 (Morris et al.,

339 2009) and AutoDock Vina 1.1.2 (Trott & Olson, 2010) were used. The procedure was carried out

340 by removing water molecules and other residues present in the target structures. A polar hydrogen

341 group was added to establish hydrogen bonds between the macromolecule and the ligand tested.

342 The grid box was chosen based on the native ligand of the macromolecules (targets). The binding

343 potency (ΔG affinity) was used to determine better molecular interactions. The results were

344 visualized using ADT and UCSF Chimera X (Pettersen et al., 2021).

345

346 **2.6. Data analysis**

347 GraphPad Prism Software Version 8.0 (San Diego, CA, USA) was used to perform the

348 statistical analysis. Initially, data were checked for deviations from the normality of variance and

349 homogeneity of variance before analysis. Normality of data was assessed using the Shapiro-Wilks

350 test, and homogeneity of variance by the Bartlett's test. Multiple comparisons were performed using

351 a one-way ANOVA and Tukey's posthoc analysis (for parametric data) or the Kruskal-Wallis test,

352 with Dunn's posthoc (for non-parametric data). Correlation analysis was performed through

353 Pearson's (parametric data) or Spearman's method (non-parametric data). Besides, the regression

354 analysis was performed when significant differences were detected between different treatments.

355 Levels of significance were set at (p) less than 0.05, 0.01, or 0.001.

356

357 **3. RESULTS AND DISCUSSION**

358 **3.1. Synthesis and characterization of SARS-CoV-2 Spike peptides**

359 Our study's first stage was to synthesize and characterize the SARS-CoV-2 Spike peptides

360 arbitrary named PSPD2001, PSPD2002, and PSPD2003. During the peptides' cleavage, we

361 performed the addition of different reaction suppressors to avoid the return of the side chain

362 protectors present in some amino acids with a reactive side chain. The results obtained in this step

363   are shown in Table 1. Regarding the mass spectrometry analysis, the spectra obtained indicated the

364   molecular mass/charge ratio (m/z) of the identified compounds, allowing us to confirm the

365   deprecated molecules' achievement. The spectra can be seen in Figure S1 (see "Supplementary

366   Material"), and Table 2 summarizes the results obtained in this step. Figure 1 also shows the

367   structural models of the PSPD2001, PSPD2002, and PSPD2003.

368

369

370

371   **Table 1**. General information on the synthesis of the peptides used in the present study.

Sequences	Codes	M.W.	Resins	Cleavage Solution
Arg-Val-Tyr-Ser-Ser-Ala-Asn-Asn-Cys-COOH	PSPD2001	1013,09	Fmoc-Cys-Wang SG*: 0,55 mmol/g	94% TFA 2,5% H$_2$O 2,5% DODT* 1% TIS*
Gln-Cys-Val-Asn-Leu-Thr-Thr-Arg-Thr-COOH	PSPD2002	1035,18	Fmoc-Thr-Wang SG: 0,55 mmol/g	94% TFA 2,5% H$_2$O 2,5% DODT 1% TIS
Asn-Asn-Ala-Thr-Asn-COOH	PSPD2003	532,51	Fmoc-Asn-Wang SG: 0,51 mmol/g	95% TFA 2,5% H$_2$O 2,5% TIS

372   M.W.: molecular weight; SG: substitution grade– Number of active sites available for the growth of the peptide chain.

373   DODT: 2,2'-(Ethylenedioxy) diethanol;TIS: triisopropylsilane; TFA: trifluoroacetic acid.

374

375   **Table 2**. Mass spectrometry analysis after peptide purification

	PSPD2001	PSPD2002	PSPD2003
M.W.	1013,09 g/mol	1035,18 g/mol	532,51 g/mol
m/z calculated	1014,09; 507,54	1036,18;518,59	533,51
m/z obtained	1013,41; 507,52	1035,41;518,96	533,04;1064,86

376   M.W.: molecular weight; PSPD2001: Arg-Val-Tyr-Ser-Ser-Ala-Asn-Asn-Cys-COOH; PSPD2002: Gln-Cys-Val-Asn-Leu-Thr-Thr-

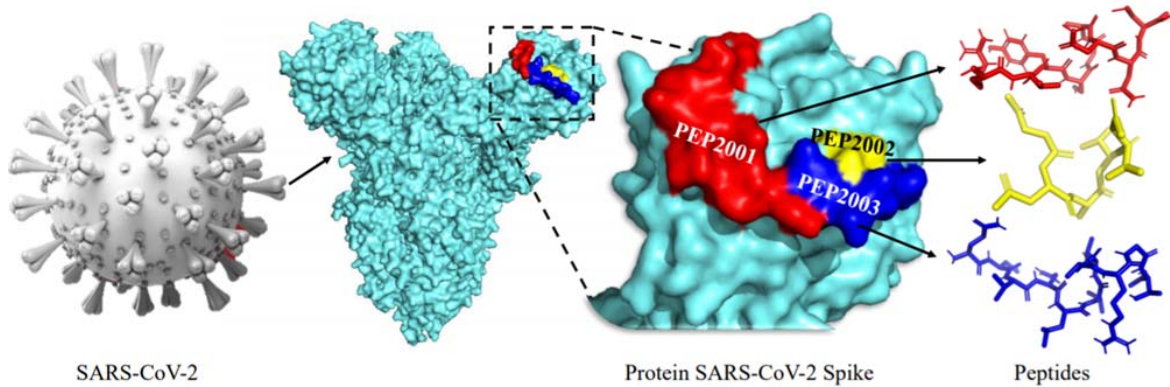377   Arg-Thr-COOH; PSPD2003: Asn-Asn-Ala-Thr-Asn-COOH.

378

379

Figure 1. Structural models of peptides (A) PSPD2001, (B) PSPD2002, and (C) PSPD2003 that were synthesized in the present study.

380

381   Regarding the alignment of the obtained sequences, our analyzes revealed the existence of

382   similarities between the nucleotide sequences of the synthesized peptides and different regions

383   conserved in SARS-Cov-2, whose comparisons were made from three datasets COVID, originated

384   from Texas (USA), Iran, and Australia (Figure 2). These data demonstrated that the peptides

385   PSPD2001, PSPD2002, and PSPD2003 are, in fact, part of the protein structure of the etiological

386   agent of COVID-19. However, the sequences obtained for *P. cuvieri* (taxid: 218685) showed two

387   main agreements belonging to five of the total of nine peptides found. The identification of possible

388   linear epitopes was performed by BLAST with the Swissprot protein sequence database restricted to

389   *P. cuvieri*. All peptides obtained in the sequencing were evaluated. However, only the main results

390   found for five peptides are being presented in Table S1, two in the form SARS-CoV-2, in addition

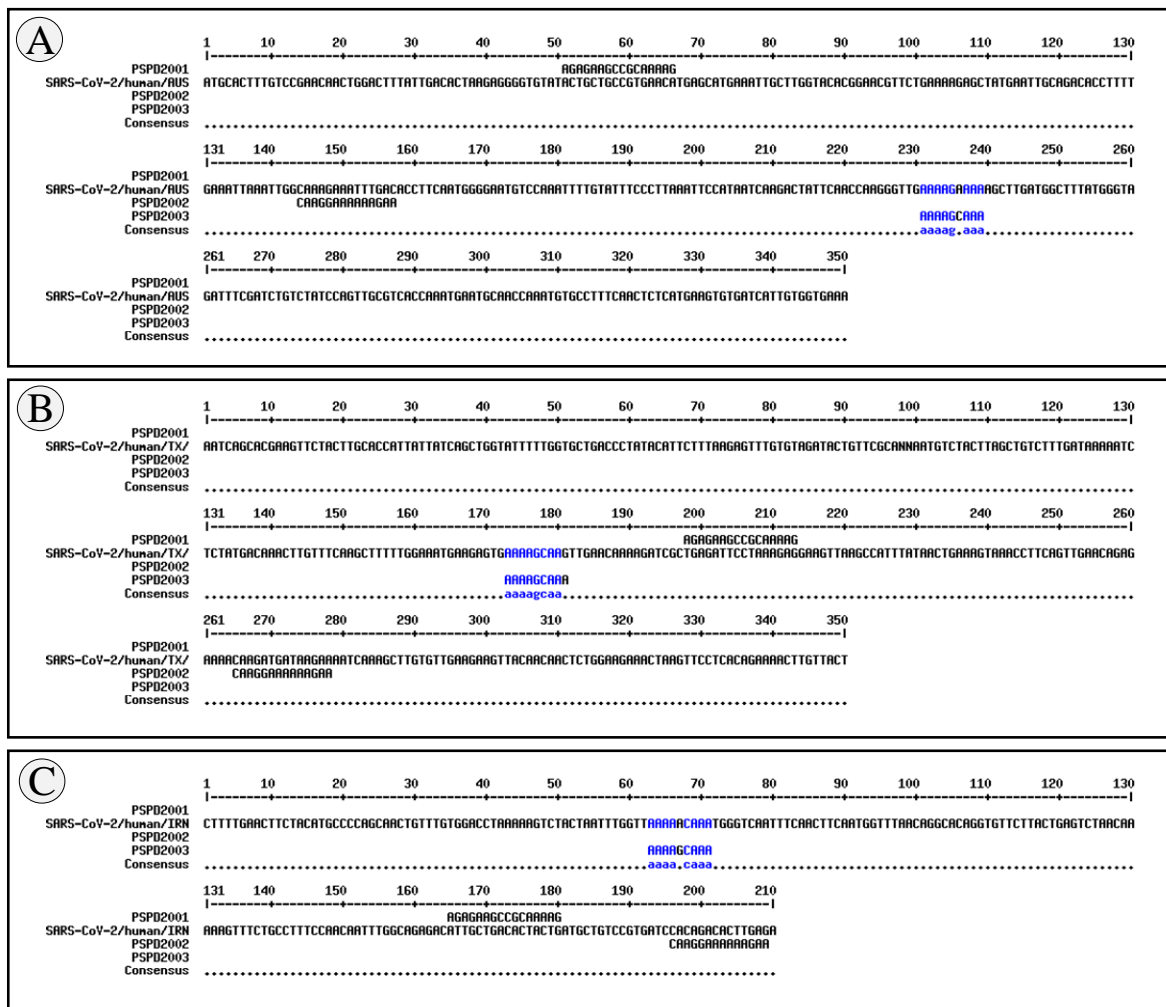391   to the analysis made for the consensus obtained in alignment with Clustal W.

Figure 2. Alignment of the nucleotide sequence encoding PSPD2001, PSPD2002 and PSPD2003 with SARS-CoV-2 obtained from the (A) COVID dataset from Australia (SARS-Cov-2 / human / AUS), (B) Texas, USA (SARS-Cov-2 / human / TX) and (C) Iran (SARS-Cov-2 / human / IRN). The blue markings refer to similar nucleotides between the synthesized peptides and those present in SARS-CoV-2.
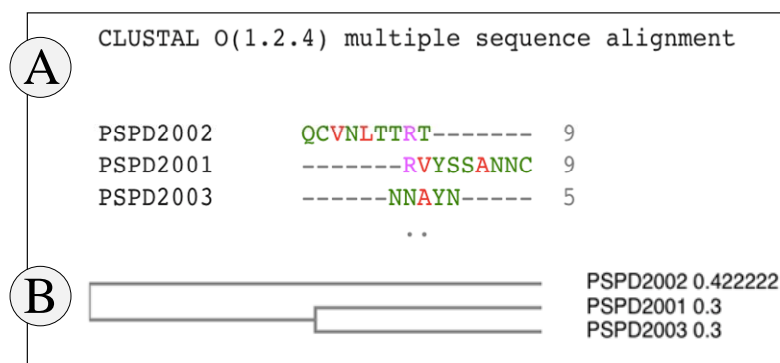
Figure 3. (A) Peptide alignment and (B) Guide Tree Phylogram. Both for the *Physalaemus cuvieri* form (taxid: 218685) by the Clustal W program. The green regions highlight 50% of the conserved region and, in red, 50% to 85% of the conserved region.

392

393   The *in vivo* experiments revealed that short exposure to SARS-CoV-2 Spike peptides was
394   able to induce significant biochemical changes in *P. cuvieri* tadpoles. After 24 h of exposure, we
395   observed that the peptides PSPD2002 and PSPD2003 (100 and 500 ng/mL) induced a significant
396   increase in nitrite production (the indirect measurement of NO (Soneja et al. 2005) and hydrogen
397   peroxide (Figure 4A-B, respectively), which in association with the higher levels of ROS (Figure
398   4D), suggest an increase in oxidative stress processes in the animals. The PSPD2003 peptide, in
399   particular, demonstrated an even more significant effect on NO production, exceeding a 30%
400   increase, to the control group, in both tested concentrations (100 and 500 ng/ml); almost 60%
401   increase in hydrogen peroxide levels in the group exposed to 500 ng/mL, and 29% ROS in the
402   animals treated with 100 ng/mL. However, we did not observe significant differences between the
403   groups regarding MDA levels (Figure S2-A), suggesting that the treatments did not intensify the
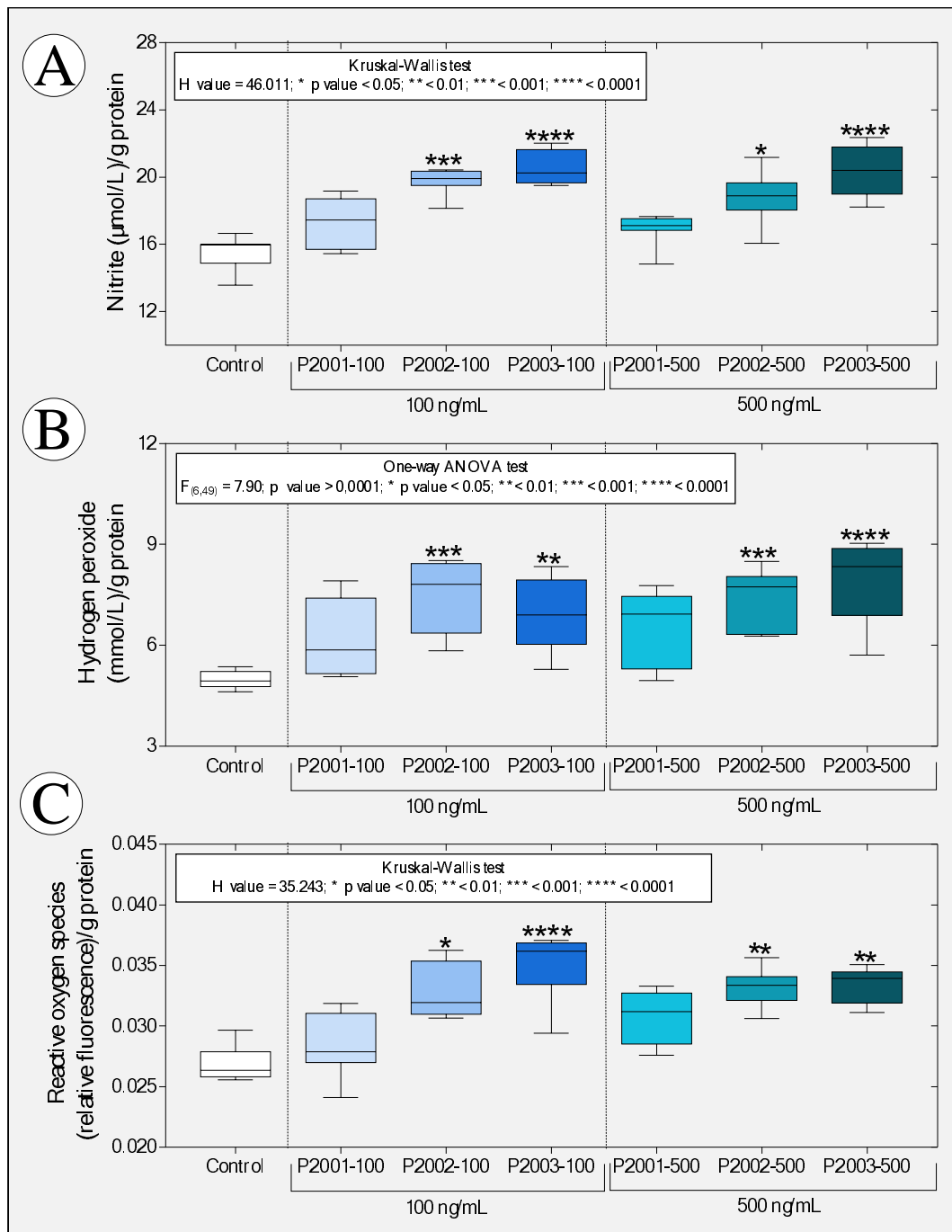404   lipid peroxidation processes in the tadpoles.

405

406

Figure 4. Boxplot of data obtained from predictive oxidative stress biomarkers [(A) nitrite levels, (B) hydrogen peroxide and (C) reactive oxygen species] in tadpoles of *P. cuvieri* (phase 27G) exposed or not to peptides PSPD 2001, 2002 and 2003 of the SARS-CoV-2 Spike protein. The summaries of the statistical analyzes are shown in the upper left corner of the graphs. Asterisks indicate significant differences between the respective groups and the control group. (n = 50 animals/group).PSPD2001: Arg-Val-Tyr-Ser-Ser-Ala-Asn-Asn-Cys- COOH; PSPD2002: Gln-Cys-Val-Asn-Leu-Thr-Thr-Arg-Thr-COOH; PSPD2003: Asn-Asn-Ala-Thr-Asn-COOH.

407   Similar to the previous findings, we observed that the animals exposed to PSPD2002 and
408   PSPD2003 showed an increase, in a concentration-dependent manner, of the activity of the
409   enzymes SOD and catalase (Figure 5A-B), with these data being positively and significantly
410   correlated with the increase in the levels of nitrite, peroxide hydrogen and ROS (Figure 5C-D). We
411   also observed that PSPD2003, once again, induced more intense effects on the antioxidant activity;
412   there was an increase above 36% as compared to the control group for the two concentrations
413   tested (100 and 500 ng/mL). The levels of SOD and catalase in the tadpoles exposed to PSPD2002
414   fragments were 28.9% higher than those reported in the control group. However, the SOD/catalase
415   ratio was unaffected or decreased which indicates the relative balance between hydrogen peroxide
416   synthesis by SOD and its decomposition by catalase (Figure 2S-B).

417   These data are exciting since they corroborate previous studies that describe the critical role
418   the SARS-CoV-2 Spike protein in inducing oxidative stress in COVID-19 infection [see the review
419   of Suhail et al. (2020)] while demonstrating that the peptides evaluated, even in a non-host
420   organism, can cause metabolic disorders related to the increase in reactive species. On the other
421   hand, the impairment of antioxidant defenses observed in several viral infections (Fraternale et al.,
422   2006), including COVID-19 (Baradaran et al., 2020; Polonikov, 2020; Bayindir & Bayindir, 2020;
423   Abouhashem et al., 2020), was not evident in the studied organism. These data also reinforce the
424   hypothesis that the responses to the peptide fragments tested may be different between hosts and
425   non-hosts of SARS-CoV-2; they also confirm the ability of peptides PSPD2002 and PSPD2003 to
426   induce metabolic changes that alter REDOX homeostasis towards oxidative stress in tadpoles.

427   The proportional increase in oxidative stress biomarkers and the activity of SOD and
428   catalase enzymes [two essential and indispensable molecules in cellular antioxidant defense
429   strategies -Nishikawa et al. (2009), Hu & Tirelli (2012) and Ighodaro & Akinloye (2018)]
430   reinforces our hypothesis, showing that the increase in antioxidant defenses does not seem to have
431   been sufficient to reduce oxidative stress. The proposition of an action mechanism explaining the
432   increase in these enzymes' activity is very incipient, either due to our study's pioneering nature or
433   the need to deepen biochemical assessments in future studies. However, it is tempting to speculate
434   that the interactions between PSPD2002 and PSPD2003 peptides and antioxidant enzymes
435   evaluated in tadpoles (confirmed by molecular docking) have induced functional changes in SOD
436   and catalase, similarly to what was observed by Jing et al. (2020) by exposing hepatocytes isolated
437   from C57BL6 mice to different concentrations of naphthalene. The data obtained from the
438   molecular docking reinforces our hypothesis by confirming the affinity between the PSPD2002 and
439   PSPD2003 peptides and the referred enzymes and the existence of interactions with residues from
440   all tested moorings (Figure 6). In the interactions with PSPD2002, it was possible to verify several

441 hydrogen bonds in the threonine mixture (T9), revealing the potencies of the binding affinities and
442 the central region of interaction in the active sites of the tested targets. In contrast, PSPD2003
443 interactions showed ≥20 hydrogen interactions in all the tested couplings, with the structures of
444 valine (V2) and serine (S4) (central of the peptide) considered to have the best affinity region of the
445 ligand.

446   An increase in NO production (inferred by high levels of nitrite) in tadpoles exposed to
447 PSPD2002 and PSPD2003 (Figure 4A) suggests that the production of this free radial gas
448 constitutes a standard response to the constituents of the SARS-CoV protein -2 Spike of the new
449 coronavirus, both in the evaluated non-host organism and in humans infected with SARS-CoV-2.
450 The ability of NO (both endogenous and exogenous) to inhibit the replication cycle of other viruses
451 in the Coronaviridae family, affecting their proteins and reducing viral RNA (Chen et al., 2004;
452 Keyaerts et al., 2004; Åkerström et al., 2005; Jung et al., 2010), has even motivated studies, whose
453 preliminary results point to its potential therapeutic use in patients infected with SARS-CoV-2
454 (Alvarez et al., 2020). Alternatively, we cannot neglect the hypothesis of increased NO in tadpoles
455 due tothe innate immune response modulated by the peptides, with a consequent increase in the
456 production of inflammatory cytokines. In this case, studies reporting a positive correlation between
457 NO production and increased pro-inflammatory cytokine levels (TNF-α, IL-6, IL-17, IL-12, and
458 interferon-γ) in patients with COVID-19 reinforce our hypothesis (Karki et al., 2020; Del Valle et
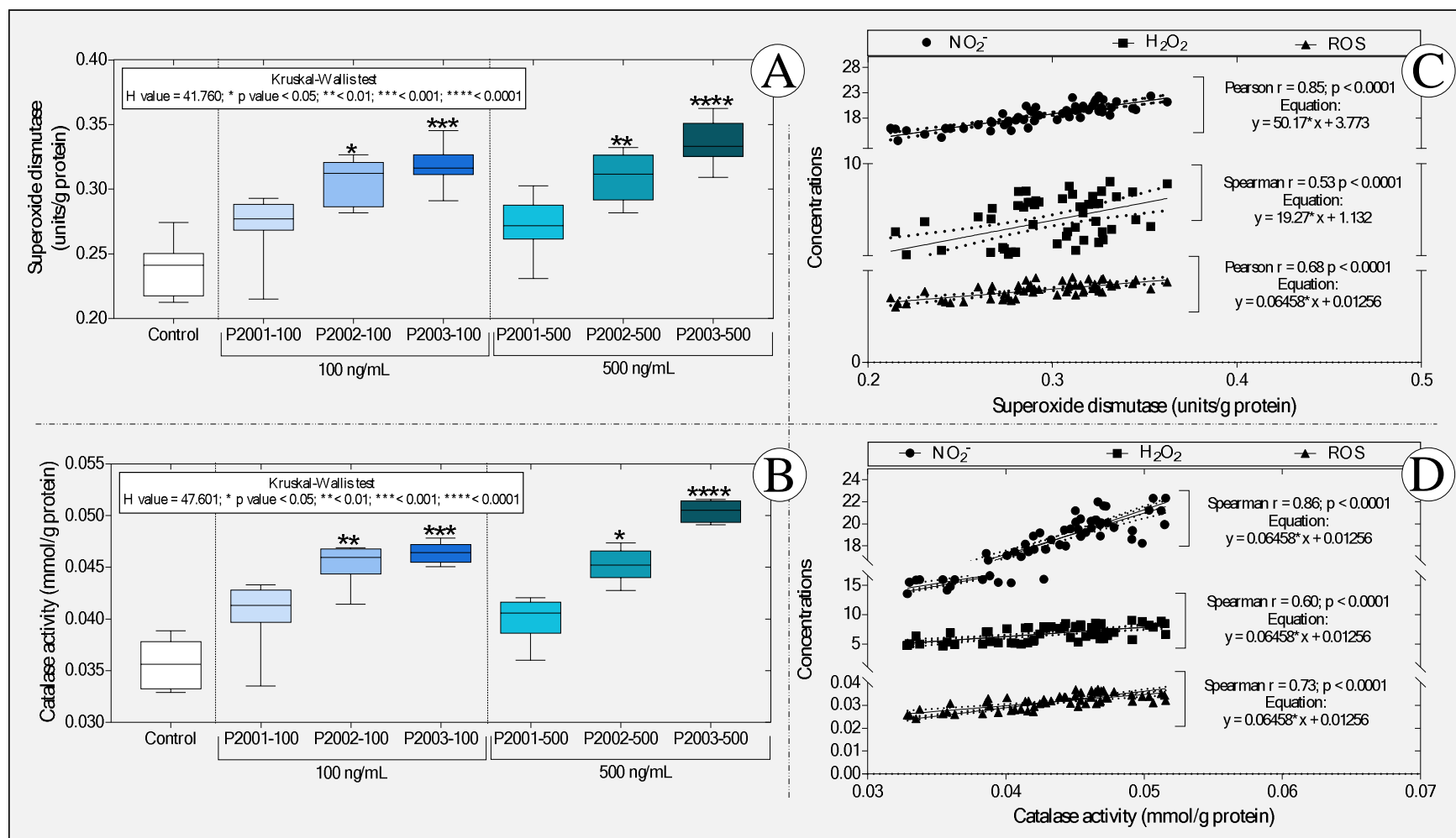459 al., 2020; Costela-Ruiz et al., 2020).

Figure 5. Boxplot of the activity of the enzymes (A) superoxide dismutase and (B) catalase, as well as correlations between the levels of (C) superoxide dismutase and (D) catalase and the different predictive biomarkers of oxidative stress. NO2-: nitrite; H2O2: hydrogen peroxide and ROS: reactive oxygen species. In "A" and "B," the statistical analyses' summaries are shown in the graphs' upper left corner. Asterisks indicate significant differences between the respective groups and the control group. (n = 50 animals / group). PSPD2001: Arg-Val-Tyr-Ser-Ser-Ala-Asn-Asn-Cys- COOH; PSPD2002: Gln-Cys-Val-Asn-Leu-Thr-Thr-Arg-Thr-COOH; PSPD2003: Asn-Asn-Ala-Thr-Asn-COOH.
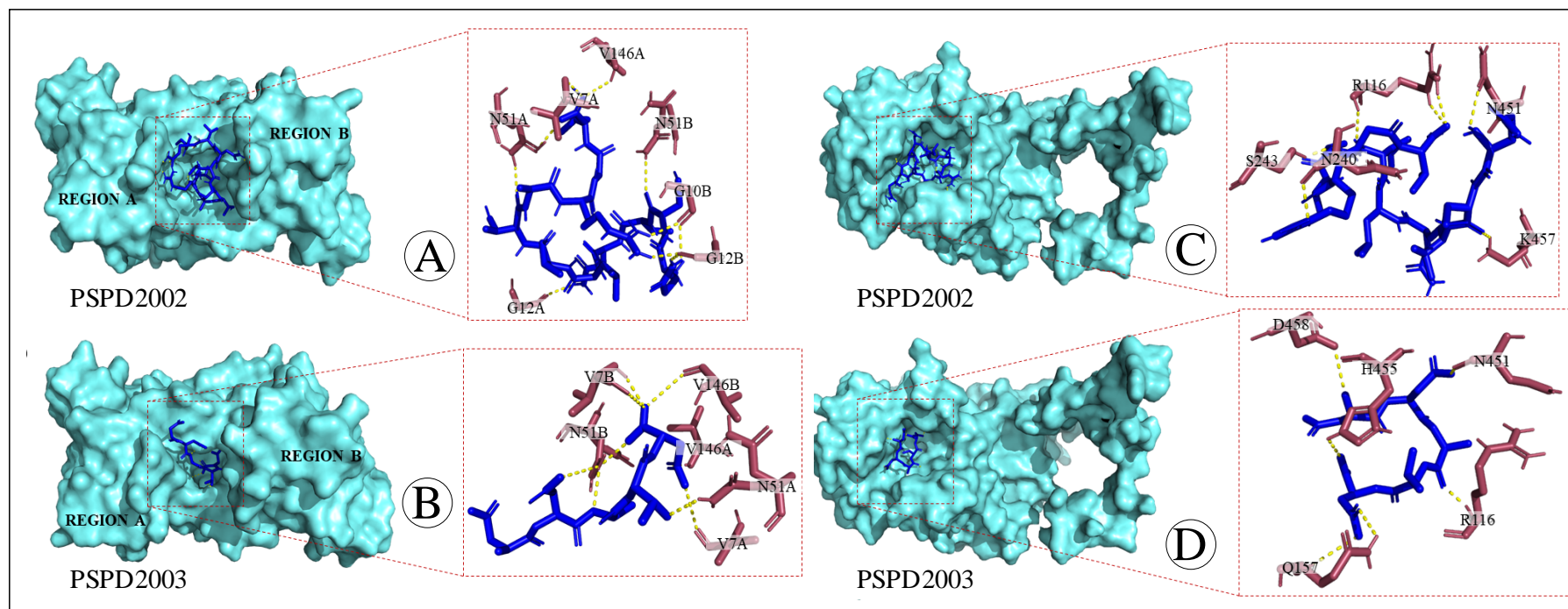
460

Figure 6. Three-dimensional surface-ligand coupling of interactions between peptides PSPD2002 and PSPD-2003 and the enzyme (A-B) superoxide dismutase (SOD) and (C-D) catalase (C-D), all in surface mode and highlighted active site. In "B and D", we also observe regions A and B of the homo-dimer structure. Interaction residues in "A" (SOD-PSPD2002): G12A; N51A *; V7A; V146B; G10B *; G12B *; N51B (affinity (kcal / mol) = -8.3). In "B" (SOD-PSPD2002): N51A; V7A; V146A; N51B **; V7B; V146B * (affinity (kcal / mol) = -8.6). In "C" (Catalase-PSPD2002): K457; N240; N451; R116 **; S243 (affinity (kcal / mol) = -9.3). In "D" (Catalase-PSPD2003): D458; H455; N451; Q157 *; R116 (affinity (kcal / mol) = -6.8). An "asterisk" indicates two interactions in the same residue. Two "asterics" indicate the existence of three interactions in the same residue.

464   We also evaluated the peptides' possible neurotoxicity in tadpoles exposed to the peptide
465   fragments of the SARS-CoV-2 Spike protein. Interestingly, we observed that 100 ng/mL PSPD2003
466   induced an increase greater than 220% concerning the control group. However, at a concentration
467   of 500 ng/mL, all the peptides evaluated exerted an effect in the cholinergic system, causing an
468   increase in the activity of AChE (Figure 7). While the peptides PSPD2001 and PSPD2002 induced
469   increases of 219 and 553.8% in relation to AChE activity in the control group's animals,
470   respectively; the PSPD2003 peptide impressively induced an even more significant increase
471   (697.3%). Therefore, these data confirmed the initial hypothesis that the SARS-CoV-2 Spike
472   fragments induce neurotoxic effects, inferred by the stimulatory effect of the cholinergic system of
473   the animals evaluated, especially in those exposed to the highest concentration (500 ng/mL) of the
474   peptides.

475
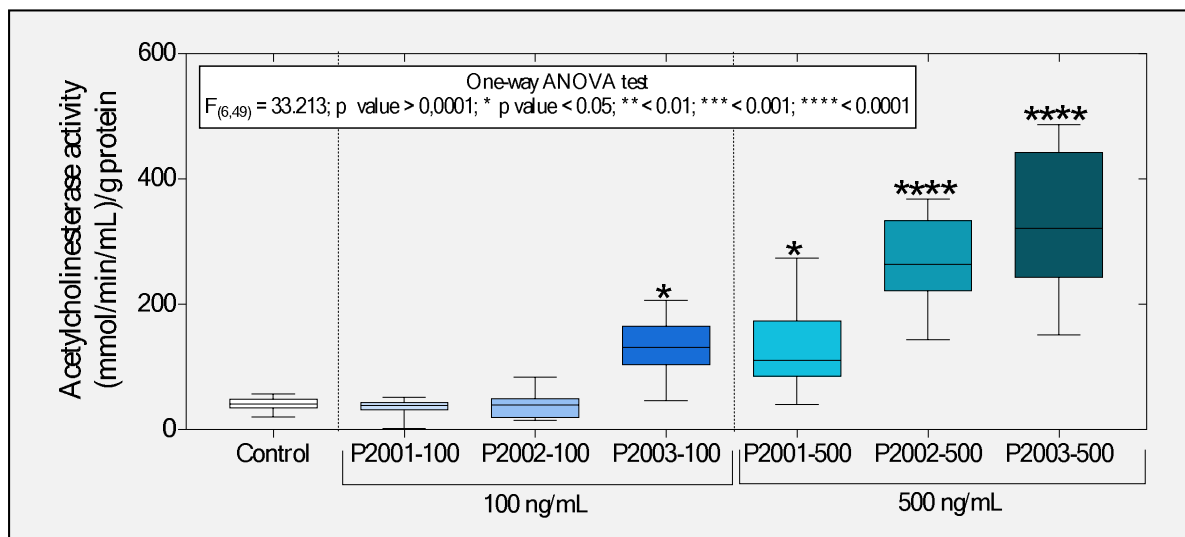
Figure 7. Boxplot of the enzyme acetylcholinesterase activity evaluated in tadpoles of P. cuvieri exposed or not to the peptides PSPD 2001, 2002, and 2003 of the SARS-CoV-2 Spike protein. The summaries of the statistical analyzes are shown in the upper left corner of the graphs. Asterisks indicate significant differences between the respective groups and the control group. (n = 50 animals / group). PSPD2001: Arg-Val-Tyr-Ser-Ser-Ala-Asn-Asn-Cys- COOH; PSPD2002: Gln-Cys-Val-Asn-Leu-Thr-Thr-Arg-Thr-COOH; PSPD2003: Asn-Asn-Ala-Thr-Asn-COOH.

476

477   Interestingly, these data differ from other studies that report suppression in AChE induced
478   by increased cellular oxidative stress (Flora et al., 2013; Kayode et al., 2016; Bali et al., 2019;
479   Ezeoyili et al., 2019; Pala et al., 2019; Ibrahim et al., 2020). In general, such studies argue that this
480   can occur due to the deterioration of neurotransmission and oxidative damage. Additionally, AChE

481   inhibition impairs oxidative phosphorylation and is followed by neuronal Ca^{2+} influx and activation

482   of nNOS, associated with the neurons'oxidative and nitrosative injury (Milatovic et al., 2006).

483   However, the increased AChE activity observed in tadpoles exposed to the peptides may be related

484   to the activation of the cholinergic anti-inflammatory pathway (CAP), which has been found

485   beneficial in preventing inflammatory conditions such as sepsis and acute respiratory distress

486   syndrome in animal models [see the review of Liu et al. (2020)]. As discussed by Osman (2020),

487   CAP constitutes a neural mechanism that modulates inflammation through the release of

488   acetylcholine (ACh), that have led to increased AChE synthesis to decompose higher levels of this

489   neurotransmitter [see details in Tracey (2007)]. This mechanism has been reported in different

490   studies involving patients infected with the new coronavirus (Bonaz et al., 2020; Mazloom et al.,

491   2020; Pomara et al., 2020), strengthening the presumption that this mechanism may constitute

492   another similar physiological response between SARS-CoV-2 non-host and host organisms. Besides,

493   it is plausible to assume not only that the peptide composition of the SARS-CoV-2 Spike protein

494   participates in the CAP activation (both in humans and in the evaluated tadpoles) but also that the

495   neuroimmune system of the tadpoles has an essential role in responding to exposure of peptides

496   PSPD2001, PSPD2002 and PSPD2003.

497   Alternatively, the tadpoles' cholinergic system's stimulation may also be explained by the

498   direct interactions between the tested peptides and AChE, whose affinity was demonstrated in the

499   molecular docking analysis (Figure 8). In this case, future studies will be useful to understand if

500   these interactions induced a significant change in the association and catalysis mechanism or

501   expansion of the enzyme efficiency with an increase of the substrate affinity to the active site

502   (increasing the catalytic constant was increased and decreasing the Michaelis constant). In both

503   situations, a significant increase in AChE activity can occur, either as part of a compensatory

504   mechanism that will aim to compensate for the enzyme's catalytic deficit or as a more efficient

505   response to the increased release of acetylcholine in synaptic clefts via CAP activation. The

506   hypothesis that increased AChE activity in these animals was associated with positive AChE gene

507   regulation due to Spike protein peptides' inhibitory effect needs to be tested in future studies.

508   Finally, it is essential to emphasize that although our study gathers clear and pioneering

509   evidence on the negative impact of the SARS-CoV-2 Spike fragments (especially PSPD2002 and

510   PSPD2003) on the biochemical parameters evaluated in *P. cuvieri* tadpoles, many questions about

511   the consequences of the presence of these fragments in the aquatic environment remains obscure.

512   The evaluation of the effects of prolonged exposure to the tested peptides (in higher and lower

513   concentrations), the use of other experimental models (expanding the environmental

514   representativeness), and the use of multiple toxicity biomarkers are some future investigative

515 perspectives. Equally important will be to deepen the mechanisms of action of the peptides of the

516 SARS-CoV-2 Spike protein when in direct contact with non-host organisms of the new coronavirus.

517 Approaches of this nature can significantly expand our knowledge of the impact of COVID-19 on

518 the environment and the functioning of ecosystems, and support the proposal for strategies to

519 remedy or mitigate aquatic contamination by SARS-Cov2 particles.
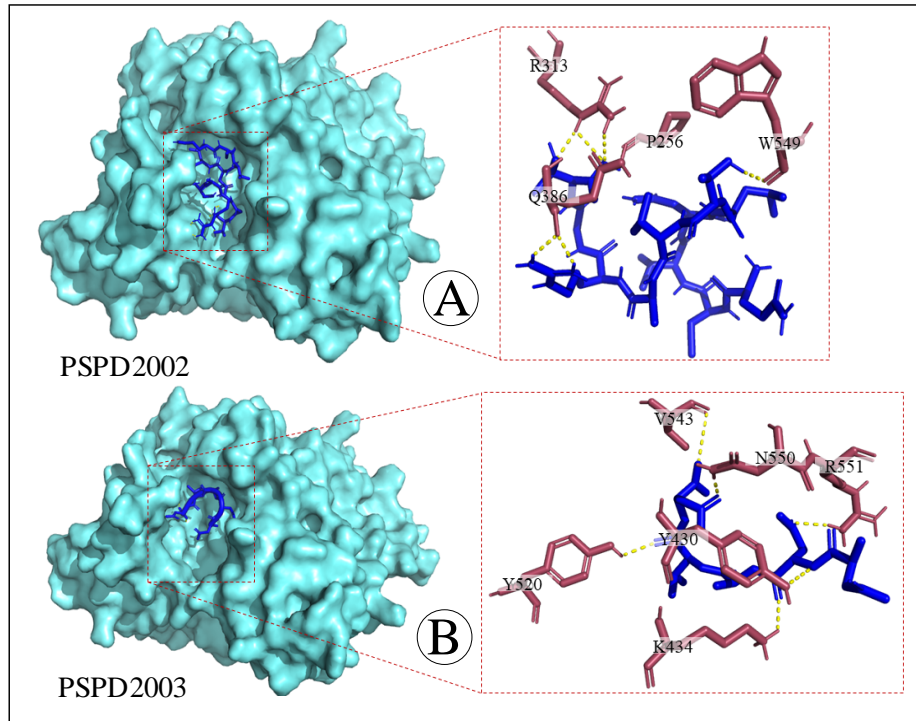
520

Figure 8. Three-dimensional surface-ligand coupling of interactions between peptides (A) PSPD2002 and (B) PSPD-2003 and the enzyme acetylcholinesterase, all in surface mode and highlighted active site. Interaction residues in "A" (AChE-PSPD2002): P256; Q386 *; R313 **; W549 (affinity (kcal / mol) = -9.4). In "B" (AChE-PSPD2003): K434; N550; R551; V543; Y430; Y520 (affinity (kcal / mol) = -8.4). An "asterisk" indicates two interactions in the same residue. Two "asterics" indicate the existence of three interactions in the same residue.

521

522 **4. CONCLUSIONS**

523 From a systemic approach that included the synthesis, cleavage, purification, and alignment

524 of peptides to *P. cuvieri* tadpoles' exposure to peptide fragments of Spike protein, we gathered

525 evidence that confirms the toxicity of viral constituents in the evaluated animal model. The

526 increase in predictive biomarkers of REDOX imbalance and neurotoxic action is, therefore, an

527 insight into how aquatic particle contamination of SARS-CoV-2 can constitute additional

528 environmental damage to the COVID-19 pandemic. In this sense, we strongly suggest conducting

529 further studies necessary to understand the real magnitude of the biological/environmental impact
530 of COVID-19.

531

537

538 **6. REFERENCES**
539 Abouhashem, A. S., Singh, K., Azzazy, H. M., & Sen, C. K. (2020). Is Low Alveolar Type II Cell
540   SOD3 in theLungsofElderlyLinkedtotheObservedSeverity of COVID-19?.Antioxidants&
541   Redox Signaling.
542 Abu-Qdais, H. A., Al-Ghazo, M. A., & Al-Ghazo, E. M. (2020). Statistical analysis and
543   characteristics of hospital medical waste under novel Coronavirus outbreak. Global Journal
544   of Environmental Science and Management, 6(Special Issue (Covid-19)), 21-30.
545 Abu-Rayash, A., &Dincer, I. (2020). Analysis of the electricity demand trends amidst the COVID-
546   19 coronavirus pandemic. Energy Research & Social Science, 68, 101682.
547 AdrieliSachett, Matheus Gallas-Lopes, Greicy M MConterato, RadharaniBenvenutti , Ana P
548   Herrmann, Angelo Piato 2020. Quantification of thiobarbituric acid reactive species
549   (TBARS) optimized for zebrafish brain tissue. protocols.io.
550   https://dx.doi.org/10.17504/protocols.io.bjp8kmrw
551 Åkerström, S., Gunalan, V., Keng, C. T., Tan, Y. J., &Mirazimi, A. (2009). Dual effectofnitric oxide
552   on SARS-CoVreplication: viral RNA production and palmitoylationofthe S protein are
553   affected. Virology, 395(1), 1-9.
554 Åkerström, S., Mousavi-Jazi, M., Klingström, J., Leijon, M., Lundkvist, Å., &Mirazimi, A. (2005).
555   Nitric oxide inhibitsthereplicationcycleofsevereacuterespiratorysyndrome coronavirus.
556   Journal of virology, 79(3), 1966-1969.
557 Alvarez RA, Berra L, Gladwin MT. Home nitric oxide therapyfor COVID-19. Am J
558   RespirCritCareMed, 202(1): 16-20, 2020.
559 Araújo, A. P. C., de Melo, N. F. S., de Oliveira Junior, A. G., Rodrigues, F. P., Fernandes, T., de
560   Andrade Vieira, J. E., ... &Malafaia, G. (2020a). How much are microplastics harmful to
561   the health of amphibians? A study with pristine polyethylene microplastics and
562   Physalaemus cuvieri. Journal of hazardous materials, 382, 121066.

563 Araújo, A. P. C., Gomes, A. R., & Malafaia, G. (2020b). Hepatotoxicity of pristine polyethylene
564   microplastics in neotropical physalaemus cuvieri tadpoles (Fitzinger, 1826). Journal of
565   Hazardous Materials, 386, 121992.

566 Bali, Y. A., Kaikai, N. E., Ba-M'hamed, S., & Bennis, M. (2019). Learning and
567   memoryimpairmentsassociatedtoacetylcholinesteraseinhibition and oxidative stress
568   followingglyphosatebased-herbicideexposure in mice. Toxicology, 415, 18-25.

569 Bangaru, S., Ozorowski, G., Turner, H. L., Antanasijevic, A., Huang, D., Wang, X., ... & Patel, N.
570   (2020). Structural analysis of full-length SARS-CoV-2 spike protein from an advanced
571   vaccine candidate. Science, 370(6520), 1089-1094.

572 Baradaran, A., Ebrahimzadeh, M. H., Baradaran, A., &Kachooei, A. R. (2020).
573   Prevalenceofcomorbidities in COVID-19 patients: A systematicreview and meta-analysis.
574   Archives ofBone and JointSurgery, 8(Suppl 1), 247.

575 Bayindir, M., &Bayindir, E. E. (2020). Synergic viral-bacterialco-infection in catalase-deficient
576   COVID-19 patients causes suppressedinnateimmunity and
577   lungdamagesduetodetrimentalelevationofhydrogenperoxideconcentration. Available at
578   SSRN 3648292.

579 Behrendt, R., White, P., & Offer, J. (2016). Advances in Fmoc solid‐phase peptide synthesis.
580   Journal of Peptide Science, 22(1), 4-27.

581 Bivins, A., Greaves, J., Fischer, R., Yinda, K. C., Ahmed, W., Kitajima, M., ... & Bibby, K. (2020).
582   Persistence of SARS-CoV-2 in water and wastewater. Environmental Science &
583   Technology Letters.

584 Blaustein, A. R., &Kiesecker, J. M. (2002). Complexity in conservation: lessons from the global
585   decline of amphibian populations. Ecology letters, 5(4), 597-608.

586 Bonaz, B., Sinniger, V., & Pellissier, S. (2020). Targetingthecholinergicanti-
587   inflammatorypathwaywithvagusnervestimulation in patientswith Covid-19?.Bioelectronic
588   medicine, 6(1), 1-7.

589 Braz HLB, Silveira JAM, Marinho AD, de Moraes MEA, Moraes Filho MO, Monteiro HSA, Jorge
590   RJB. In silico study of azithromycin, chloroquine and hydroxychloroquine and their
591   potential mechanisms of action against SARS-CoV-2 infection. Int J AntimicrobAgents.
592   2020 Sep;56(3):106119. doi: 10.1016/j.ijantimicag.2020.106119. Epub 2020 Jul 30. PMID:
593   32738306; PMCID: PMC7390782.

594 Carvalho, M., Bandeira de Mello Delgado, D., de Lima, K. M., de Camargo Cancela, M., dos
595   Siqueira, C. A., & de Souza, D. L. B. (2020). Effects of the COVID‐19 pandemic on the

596   Brazilian electricity consumption patterns. International Journal of Energy Research,
597   e5877.

598 Chen L, Liu P, Gao H, Sun B, Chao D, et al. (2004) Inhalationofnitric oxide in
599   thetreatmentofsevereacuterespiratorysyndrome: a rescue trial in Beijing. Clin InfectDis 39:
600   1531-1535.

601 Chen, Y., Chen, L., Deng, Q., Zhang, G., Wu, K., Ni, L., ... & Yang, J. (2020). The presence of
602   SARS□CoV□2 RNA in the feces of COVID□19 patients. Journal of medical virology.

603 Colston, J. T., Chandrasekar, B., & Freeman, G. L. (2002). A novel peroxide-
604   inducedcalciumtransientregulates interleukin-6 expression in cardiac-derivedfibroblasts.
605   Journal of BiologicalChemistry, 277(26), 23477-23483.

606 Costela-Ruiz, V. J., Illescas-Montes, R., Puerta-Puerta, J. M., Ruiz, C., & Melguizo-Rodríguez, L.
607   (2020). SARS-CoV-2 infection: the role ofcytokines in COVID-19 disease.
608   Cytokine&Growth Factor Reviews.

609 Coughlan, L. (2020). Snatching the Crown from SARS-CoV-2. Cell Host & Microbe, 28(3), 360-
610   363.

611

612 Chakraborty, I & Prasenjit, M. COVID-19 outbreak: Migration, effects on society, global
613   environment and prevention. Science of the Total Environment, 2020, 138882.

614

615 Del Valle, D. M., Kim-Schulze, S., Hsin-hui, H., Beckmann, N. D., Nirenberg, S., Wang, B., ...
616   &Marron, T. (2020). Aninflammatorycytokinesignaturehelpspredict COVID-19 severity
617   and death. medRxiv.

618 Del-Maestro, R. F., & McDonald, W. (1985). Oxidative enzymes in tissue homogenates. Handbook
619   of methods for oxygen radical research, 291-296.

620 Elnemma, E. M. (2004). Spectrophotometric determination of hydrogen peroxide by a
621   hydroquinone-aniline system catalyzed by molybdate. Bulletin of the Korean Chemical
622   Society, 25(1), 127-129.

623 Elsamadony, M., Fujii, M., Miura, T., & Watanabe, T. (2020). Possible transmission of viruses from
624   contaminated human feces and sewage: Implications for SARS-CoV-2. Science of the
625   Total Environment, 755, 142575.

626 Emmanuel DaanobaSunkari, Harriet MatekoKorboe, Mahamuda Abu, TefideKizildeniz,

627 Estrela, F. N., Guimarães, A. T. B., Silva, F. G., da Luz, T. M., Silva, A. M., Pereira, P. S., &
628   Malafaia, G. (2021). Effects of polystyrene nanoplastics on Ctenopharyngodonidella (grass

629   carp) after individual and combined exposure with zinc oxide nanoparticles. Journal of
630   Hazardous Materials, 403, 123879.

631   European Centre for Disease Prevention and Control (ECDC). **COVID-19 situation update for the**
632   EU/EEA   and   the   UK,   as   of   week   50   2020.   Available   in:
633   https://www.ecdc.europa.eu/en/cases-2019-ncov-eueea. Acesson: 21 december 2020.

634

635   Editorital, The Lancet Respiratory Medicine, COVID-19 transmission—up in the air,
636   The Lancet Respiratory Medicine,Volume 8, Issue 12, 2020, Page 1159,ISSN 2213-2600,
637   https://doi.org/10.1016/S2213-2600(20)30514-2.

638   Ezeoyili, I. C., Mgbenka, B. O., Atama, C. I., Ngwu, G. I., Madu, J. C., &Nwani, C. D. (2019).
639   Changes   in   BrainAcetylcholinesterase   and   Oxidative   Stress   Biomarkers   in
640   AfricanCatfishExposedtoCarbendazim. JournalofAquatic Animal Health, 31(4), 371-379.

641   Farsalinos, K., Niaura, R., Le Houezec, J., Barbouni, A., Tsatsakis, A., Kouretas, D., ... &Poulas, K.
642   (2020). Nicotine and SARS-CoV-2: COVID-19 may be a disease of the nicotinic
643   cholinergic system. Toxicology Reports.

644   Fernandes, BH, Feitosa, N. M., Barbosa, A. P., Bomfim, C. G., Garnique, A. M. B., Gomes, F. I. F.,
645   ... & Charlie-Silva, I. (2020). Zebrafish studies on the vaccine candidate to COVID-19, the
646   Spike   protein: Production   of   antibody   and   adverse   reaction.
647   https://doi.org/10.1101/2020.10.20.346262

648   Flora, S. J., Mehta, A., Satsangi, K., Kannan, G. M., & Gupta, M. (2003). Aluminum-
649   inducedoxidative stress in ratbrain: response tocombinedadministrationofcitricacid and
650   HEDTA. ComparativeBiochemistry and PhysiologyPart C: Toxicology&Pharmacology,
651   134(3), 319-328.

652   Fraternale A, Paoletti MF, Casabianca A, Oiry J, Clayette P, Vogel JU, Cinatl J, Jr, Palamara AT,
653   Sgarbanti R, Garaci E, Millo E, Benatti U, Magnani M. Antiviral and
654   immunomodulatorypropertiesof new pro-glutathione (GSH) molecules. CurrMedChem.
655   2006;13(15):1749–1755. doi: 10.2174/092986706777452542

656   Frost DR. Amphibian Species of the World: an Online Reference. Version 6.0. Available in:
657   http://research.amnh.org/vz/herpetology/amphibia/. Access on: 11 march. 2017.

658   Gaudin, Raphael; Goetz, Jacky G. Tracking Mechanisms of Viral Dissemination In Vivo. Trends in
659   Cell Biology, 2021.

660

661   Gornall, A.G.; Bardawill, C.J.; David, M. M. Determination of serum proteins by means of the
662   biuret reaction. J. Biol. Chem. v.177, p.751-766, 1949.

663   Gosner KL. A simplified table for staging anuran embryos and larvae with notes on identification.
664   Herpetologica, 16:183–190 1960.

665   Grant, E. H. C., Miller, D. A., &Muths, E. (2020). A Synthesis of Evidence of Drivers of Amphibian
666   Declines. Herpetologica.

667   Graham, Katherine E., et al. SARS-CoV-2 RNA in Wastewater Settled Solids Is Associated with
668   COVID-19 Cases in a Large Urban Sewershed. Environmental science & technology,
669   2020.

670   Guerrero-Latorre, L., Ballesteros, I., Villacrés-Granda, I., Granda, M. G., Freire-Paspuel, B., &Ríos-
671   Touma, B. (2020). SARS-CoV-2 in river water: Implications in low sanitation countries.
672   Science of the Total environment, 743, 140832.

673   Guimarães, A. T. B., Charlie-Silva, I., & Malafaia, G. (2020). TOXIC EFFECTS OF
674   NATURALLY-AGED MICROPLASTICS ON ZEBRAFISH JUVENILES: A MORE
675   REALISTIC APPROACH TO PLASTIC POLLUTION IN FRESHWATER
676   ECOSYSTEMS. JournalofHazardousMaterials, 124833.

677   Guimarães, A. T. B., de Lima Rodrigues, A. S., Pereira, P. S., Silva, F. G., & Malafaia, G. (2021).
678   Toxicity of polystyrene nanoplastics in dragonfly larvae: An insight on how these pollutants
679   can affect bentonic macroinvertebrates. Science of The Total Environment, 752, 141936.

680   Guy, C. A., & Fields, G. B. (1997). [5] Trifluoroacetic acid cleavage and deprotection of resin-
681   bound peptides following synthesis by Fmoc chemistry. Methods in enzymology, 289, 67-83.

682   Harrison, A. G., Lin, T., & Wang, P. (2020). Mechanisms of SARS-CoV-2 transmission and
683   pathogenesis. Trends in immunology.

684   HENRY, R. J.; SOBEL, C.; BERKMAN, S. Interferences with biuret methods for serum proteins.
685   Use of Benedict's qualitative glucose reagent as a biuret reagent. Anal. Chem. v.29, p.1491-
686   1495, 1957.

687   Herek, J. S., Vargas, L., Trindade, S. A. R., Rutkoski, C. F., Macagnan, N., Hartmann, P. A., &
688   Hartmann, M. T. (2020). Can environmental concentrations of glyphosate affect survival
689   and cause malformation in amphibians? Effects from a glyphosate-based herbicide on
690   Physalaemus cuvieri and P. gracilis (Anura: Leptodactylidae). Environmental Science and
691   Pollution Research, 1-12.

692   Higgins, D. G., Thompson, J. D., & Gibson, T. J. (1996). [22] Using CLUSTAL for multiple
693   sequence alignments. In Methods in enzymology (Vol. 266, pp. 383-402). Academic Press.

694   Hu, P., &Tirelli, N. (2012). Scavenging ROS: superoxidedismutase/catalasemimeticsbythe use
695   ofanoxidation-sensitivenanocarrier/enzymeconjugate. Bioconjugatechemistry, 23(3), 438-
696   449.

697   Huang, Y., Yang, C., Xu, X. F., Xu, W., & Liu, S. W. (2020). Structural and functional properties of
698   SARS-CoV-2 spike protein: potential antivirus drug development for COVID-19. Acta
699   PharmacologicaSinica, 41(9), 1141-1149.

700   Ibrahim, K. A. E. M., Abdelrahman, S. M., Elhakim, H. K., &Ragab, E. A. (2020).
701   Singleorcombinedexposuretochlorpyrifos and cypermethrinprovokeoxidative stress and
702   downregulation in monoamine oxidase and acetylcholinesterase gene
703   expressionoftherat'sbrain. EnvironmentalScience and PollutionResearch, 1-12.Pomara, N.,
704   &Imbimbo, B. P. (2020). Impairmentofthecholinergicanti-inflammatorypathway in
705   oldersubjectswithsevere COVID-19. Medical hypotheses.

706   Ighodaro, O. M., &Akinloye, O. A. (2018). First line defenceantioxidants-superoxidedismutase
707   (SOD), catalase (CAT) and glutathioneperoxidase (GPX): Their fundamental role in
708   theentireantioxidantdefencegrid. Alexandria journal of medicine, 54(4), 287-293.

709   Ighodaro, O. M., &Akinloye, O. A. (2018). First line defence antioxidants-superoxide dismutase
710   (SOD), catalase (CAT) and glutathione peroxidase (GPX): Their fundamental role in the
711   entire antioxidant defence grid. Alexandria journal of medicine, 54(4), 287-293.

712   Jetz, W, and R. A. Pyron. 2018. The interplay of past diversification and evolutionary isolation with
713   present imperilment across the amphibian tree of life. Nature Ecology & Evolution 2:850-
714   858.

715   Jing, M., Han, G., Wan, J., Zhang, S., Yang, J., Zong, W., ... & Liu, R. (2020). Catalase and
716   superoxidedismutase response and theunderlying molecular mechanismfornaphthalene.
717   ScienceofThe Total Environment, 139567.

718   Jones, D. L., Baluja, M. Q., Graham, D. W., Corbishley, A., McDonald, J. E., Malham, S. K., ... &
719   Wilcox, M. H. (2020). Shedding of SARS-CoV-2 in feces and urine and its potential role
720   in person-to-person transmission and the environment-based spread of COVID-19. Science
721   of the Total Environment, 749, 141364.

722   Galindo-Villegas, Jorge. The zebrafish disease and drug screening model: A strong ally against
723   Covid-19. Frontiers in Pharmacology, 2020, 11: 680.

724   Jung K, Gurnani A, Renukaradhya GJ, Saif LJ (2010) Nitric oxide iselicited and inhibits viral
725   replication in pigsinfectedwithporcinerespiratory coronavirus butnotporcinereproductive
726   and respiratorysyndrome virus. VetImmunolImmunopathol 136 335-339. [Crossref]

727   Kampf, G., Todt, D., Pfaender, S., & Steinmann, E. (2020). Persistence of coronaviruses on
728   inanimate surfaces and their inactivation with biocidal agents. Journal of Hospital
729   Infection, 104(3), 246-251.

730   Karki, R., Sharma, B. R., Tuladhar, S., Williams, E. P., Zalduondo, L., Samir, P., … &Schreiner, P.
731   (2020). Synergismof TNF-α and IFN-γtriggersinflammatorycelldeath, tissuedamage, and
732   mortality in SARS-CoV-2 infection and cytokine shock syndromes. Cell.

733   Kayode AO, Sulaiman O, Emmanuel AG, Dorcas W. Acetylcholinesteraseactivity and oxidative
734   stress indices in cerebellum, cortex and hippocampusofratsexposedto lead and manganese;
735   InternationaJournlofBiologicalResearch, 4(2): 157-164, 2016.

736   Keech, C., Albert, G., Cho, I., Robertson, A., Reed, P., Neal, S., … & Smith, G. (2020). Phase 1–2
737   trial of a SARS-CoV-2 recombinant spike protein nanoparticle vaccine. New England
738   Journal of Medicine.

739   Keyaerts E, Vijgen L, Chen L, Maes P, Hedenstierna G (2004) Inhibitionof SARS-coronavirus
740   infection in vitro by S-nitroso-N-acetylpenicillamine, a nitric oxide donorcompound. Int J
741   InfectDis. 8: 223-226. [Crossref]

742   Khan, F. R., Syberg, K., Shashoua, Y., & Bury, N. R. (2015). Influence of polyethylene microplastic
743   beads on the uptake and localization of silver in zebrafish (Danio rerio). Environmental
744   pollution, 206, 73-79.

745   Kharazmi, A., Nielsen, H., Rechnitzer, C., &Bendtzen, K. (1989). Interleukin 6 primes human
746   neutrophil and monocyteoxidativeburst response. Immunologyletters, 21(2), 177-184.

747   Klaassen, N., Spicer, V., &Krokhin, O. V. (2019). Universal retention standard for peptide
748   separations using various modes of high-performance liquid chromatography. Journal of
749   Chromatography A, 1588, 163-168.

750   Kolb, P., Ferreira, R. S., Irwin, J. J., & Shoichet, B. K. (2009). Docking and chemoinformatic
751   screens for new ligands and targets. Current opinion in biotechnology, 20(4), 429-436.

752   Lamiable A, Thévenet P, Rey J, Vavrusa M, Derreumaux P, Tufféry P. PEP-FOLD3: previsão de
753   estrutura de novo mais rápida para peptídeos lineares em solução e em complexo.
754   NucleicAcids Res. 8 de julho de 2016; 44 (W1): W449-54.

755   Li, Y., Hu, Y., Yu, J., & Ma, T. (2020). Retrospectiveanalysisoflaboratorytesting in 54
756   patientswithsevere-orcritical-type 2019 novel coronavirus pneumonia.
757   LaboratoryInvestigation, 1-7.

758   Liu, D., Thompson, J. R., Carducci, A., & Bi, X. (2020). Potential secondary transmission of SARS-
759   CoV-2 via wastewater. Science of The Total Environment, 749, 142358.

760   Liu, H., Wu, J., Yao, J. Y., Wang, H., & Li, S. T. (2017). The role ofoxidative stress in
761   decreasedacetylcholinesteraseactivity at the neuromuscular junctionofthediaphragmduring
762   sepsis. Oxidative medicine and cellularlongevity, 2017.

763   Liu, W., Liu, Z., & Li, Y. C. (2020). COVID-19-related myocarditis and cholinergicanti-
764   inflammatorypathways. HellenicJournalofCardiology.

765   Luna, O. F., Gomez, J., Cárdenas, C., Albericio, F., Marshall, S. H., & Guzmán, F. (2016).
766   Deprotection reagents in Fmoc solid phase peptide synthesis: moving away from
767   piperidine?. Molecules, 21(11), 1542.

768   Lusher, A. L., Mchugh, M., & Thompson, R. C. (2013). Occurrence of microplastics in the
769   gastrointestinal tract of pelagic and demersal fish from the English Channel. Marine
770   pollution bulletin, 67(1-2), 94-99.

771   Maharajan, K., Muthulakshmi, S., Nataraj, B., Ramesh, M., &Kadirvelu, K. (2018). Toxicity
772   assessment of pyriproxyfen in vertebrate model zebrafish embryos (Danio rerio): a multi
773   biomarker study. Aquatic Toxicology, 196, 132-145.

774   Mazloom, R. (2020). FeasibilityofTherapeuticEffectsoftheCholinergic Anti-InflammatoryPathwayon
775   COVID-19 Symptoms. Journal of NeuroimmunePharmacology, 1-2.

776   Metzger, J. W., Kempter, C., Wiesmuller, K. H., & Jung, G. (1994). Electrospray mass spectrometry
777   and tandem mass spectrometry of synthetic multicomponent peptide mixtures:
778   determination of composition and purity. Analytical biochemistry, 219(2), 261-277.

779   Meyerowitz, E. A., Richterman, A., Gandhi, R. T., & Sax, P. E. (2020). Transmission of SARS-
780   CoV-2: a review of viral, host, and environmental factors. Annals of internal medicine.

781   Milatovic, D., Gupta, R. C., & Aschner, M. (2006). Anticholinesterasetoxicity and oxidative stress.
782   TheScientificWorldJournal, 6.

783   Miranda NEO, Maciel NM, Ribeiro MSL, Colli GR, Haddad FB, Collevatti RG. Diversification of
784   the widespread neotropical frog Physalaemus cuvieri in response to Neogene-Quaternary
785   geological events and climate dynamics. Molecular Phylogeneticsand Evolution, 132: 67-
786   80, 2019.

787   Montalvão, M. F., Guimarães, A. T. B., de Lima Rodrigues, A. S., & Malafaia, G. (2021). Carbon
788   nanofibers are bioaccumulated in Aphyllawilliamsoni (Odonata) larvae and cause REDOX
789   imbalance and changes of acetylcholinesterase activity. Science of The Total Environment,
790   143991.

791   Nishikawa, M., Hashida, M., &Takakura, Y. (2009). Catalasedeliveryforinhibiting ROS-
792   mediatedtissueinjury and tumor metastasis. Advanceddrugdeliveryreviews, 61(4), 319-326.

793   Ohkawa, H., Ohishi, N., & Yagi, K. (1979). Assay for lipid peroxides in animal tissues by
794   thiobarbituric acid reaction. Analytical biochemistry, 95(2), 351-358.

795   Osman, A. H. (2020). COVID-19: Targetingthecytokinestormviacholinergicanti-inflammatory
796   (Pyridostigmine). Int. J. Clin. Virol, 4, 041-046.

797   Osman, A. H. (2020). COVID-19: Targeting the cytokine storm via cholinergic anti-inflammatory
798   (Pyridostigmine). Int. J. Clin. Virol, 4, 041-046.
799   Pais, F. S. M., de Cássia Ruy, P., Oliveira, G., & Coimbra, R. S. (2014). Assessing the efficiency of
800   multiple sequence alignment programs. Algorithms for molecular biology, 9(1), 4.
801   Pala, A. (2019). Theeffectof a glyphosate-basedherbicideonacetylcholinesterase (AChE) activity,
802   oxidative   stress,   and   antioxidantstatus   in   freshwateramphipod: Gammaruspulex
803   (Crustacean). EnvironmentalScience and PollutionResearch, 26(36), 36869-36877.
804   Pandey, D., Verma, S., Verma, P., Mahanty, B., Dutta, K., Daverey, A., & Arunachalam, K. (2020).
805   SARS-CoV-2 in wastewater: Challenges for developing countries. International journal of
806   hygiene and environmental health, 113634.
807   Pechmann, J. H., Scott, D. E., Semlitsch, R. D., Caldwell, J. P., Vitt, L. J., & Gibbons, J. W. (1991).
808   Declining amphibian populations: the problem of separating human impacts from natural
809   fluctuations. Science, 253(5022), 892-895.
810   Pettersen, EF, Goddard, TD, Huang, CC, et al. UCSF ChimeraX: Structure visualization for
811   researchers,   educators,   and   developers.   Protein   Science.   2021;   30:   70– 82.
812   https://doi.org/10.1002/pro.3943
813   Polo, D., Quintela-Baluja, M., Corbishley, A., Jones, D. L., Singer, A. C., Graham, D. W.,
814   &Romalde, J. L. (2020). Making waves: Wastewater-based epidemiology for SARS-CoV-
815   2–Developing robust approaches for surveillance and prediction is harder than it looks.
816   Water Research.
817   Polonikov,   A.   (2020).   EndogenousDeficiencyofGlutathione   as   theMostLikely   Cause
818   ofSeriousManifestations and Death in COVID-19 Patients. ACS InfectiousDiseases.
819   Pupin, N. C., Gasparini, J. L., Bastos, R. P., Haddad, C. F., & Prado, C. (2010). Reproductive
820   biology of an endemic Physalaemus of the Brazilian Atlantic forest, and the trade-off between
821   clutch and egg size in terrestrial breeders of the P. signifer group. The Herpetological Journal,
822   20(3), 147-156.
823   Qi, X., Ke, B., Feng, Q., Yang, D., Lian, Q., Li, Z., ... & Liao, G. (2020). Construction and
824   immunogenic studies of a mFc fusion receptor binding domain (RBD) of spike protein as a
825   subunit vaccine against SARS-CoV-2 infection. Chemical Communications, 56(61), 8683-
826   8686.
827   Raibaut, L., El Mahdi, O., & Melnyk, O. (2014). Solid phase protein chemical synthesis. In Protein
828   Ligation and Total Synthesis II (pp. 103-154). Springer, Cham.

829   Ranvestel, A. W., Lips, K. R., Pringle, C. M., Whiles, M. R., & Bixby, R. J. (2004). Neotropical
830   tadpoles influence stream benthos: evidence for the ecological consequences of decline in
831   amphibian populations. Freshwater Biology, 49(3), 274-285.

832   Ravichandran, S., Coyle, E. M., Klenow, L., Tang, J., Grubbs, G., Liu, S., ... & Khurana, S. (2020).
833   Antibody signature induced by SARS-CoV-2 spike protein immunogens in rabbits. Science
834   Translational Medicine.

835   Ro, J. H., Liu, C. C., & Lin, M. C. (2020). Resveratrol Mitigates Cerebral Ischemic Injury by
836   Altering Levels of Trace Elements, Toxic Metal, Lipid Peroxidation, and Antioxidant
837   Activity. Biological Trace Element Research, 1-10.

838   Rutkoski, C. F., Macagnan, N., Folador, A., Skovronski, V. J., do Amaral, A. M., Leitemperger, J.
839   W., ... & Hartmann, M. T. (2020). Cypermethrin-and fipronil-based insecticides cause
840   biochemical changes in Physalaemusgracilis tadpoles. Environmental Science and Pollution
841   Research, 1-11.

842   Sachett, A., Bevilaqua, F., Chitolina, R., Garbinato, C., Gasparetto, H., Dal Magro, J., ... & Siebel,
843   A. M. (2018). Ractopamine hydrochloride induces behavioral alterations and oxidative
844   status imbalance in zebrafish. Journal of Toxicology and Environmental Health, Part A,
845   81(7), 194-201.

846   Samrat, S. K., Tharappel, A. M., Li, Z., & Li, H. (2020). Prospect of SARS-CoV-2 spike protein:
847   Potential role in vaccine and therapeutic development. Virus research, 198141.

848   Sangkham, S. (2020). Face mask and medical waste disposal during the novel COVID-19 pandemic
849   in Asia. Case Studies in Chemical and Environmental Engineering, 2, 100052.

850   Santiago, I., Moreno-Munoz, A., Quintero-Jiménez, P., Garcia-Torres, F., & Gonzalez-Redondo, M.
851   J. (2020). Electricity demand during pandemic times: The case of the COVID-19 in Spain.
852   Energy policy, 148, 111964.

853   Sharma, H. B., Vanapalli, K. R., Cheela, V. S., Ranjan, V. P., Jaglan, A. K., Dubey, B., ... &
854   Bhattacharya, J. (2020). Challenges, opportunities, and innovations for effective solid waste
855   management during and post COVID-19 pandemic. Resources, conservation and recycling,
856   162, 105052.

857   Shutler, J., Zaraska, K., Holding, T. M., Machnik, M., Uppuluri, K., Ashton, I., ... & Dahiya, R.
858   (2020). Risk of SARS-CoV-2 infection from contaminated water systems. MedRxiv.

859   Silva, F. F. D., Silva, J. M. D., Silva, T. D. J. D., Tenorio, B. M., Tenorio, F. D. C. A. M., Santos, E.
860   L., ... & Soares, E. C. (2020). Evaluation of Nile tilapia (Oreochromis niloticus) fingerlings
861   exposed to the pesticide pyriproxyfen. Latin american journal of aquatic research, 48(5),
862   826-835.

863 Suhail, S., Zajac, J., Fossum, C., Lowater, H., McCracken, C., Severson, N., ... &Bhattacharyya, S.
864   (2020). Role ofOxidative Stress on SARS-CoV (SARS) and SARS-CoV-2 (COVID-19)
865   Infection: A Review. Theproteinjournal, 1-13.

866 Tougu, V. (2001). Acetylcholinesterase: mechanism of catalysis and inhibition. Current Medicinal
867   Chemistry-Central Nervous System Agents, 1(2), 155-170.

868 Tracey KJ. Physiology and immunologyofthecholinergicanti-inflammatorypathway. J Clin Invest.
869   2007; 117: 289-296.

870 Tran, H. N., Le, G. T., Nguyen, D. T., Juang, R. S., Rinklebe, J., Bhatnagar, A., ... & Chao, H. P.
871   (2020). SARS-CoV-2 coronavirus in water and wastewater: A critical review about
872   presence and concern. Environmental Research, 110265.

873 Trott, O; Olson, A.J. AutoDock Vina: improving the speed and accuracy of docking with a new
874   scoring function, efficient optimization, and multithreading. J Comput Chem.
875   2010;31(2):455-461. doi:10.1002/jcc.21334

876 Tsujimoto, M., Yokota, S., Vilček, J., &Weissmann, G. (1986). Tumor necrosis factor
877   provokessuperoxideaniongenerationfromneutrophils.   Biochemical   and
878   biophysicalresearchcommunications, 137(3), 1094-1100.

879 Urban, R. C., & Nakada, L. Y. K. (2021). COVID-19 pandemic: Solid waste and environmental
880   impacts in Brazil. Science of the Total Environment, 755, 142471.

881 Valavanidis, A., Vlahogianni, T., Dassenakis, M., &Scoullos, M. (2006). Molecular biomarkers of
882   oxidative stress in aquatic organisms in relation to toxic environmental pollutants.
883   Ecotoxicology and environmental safety, 64(2), 178-189.

884 Wang, X. W., Li, J. S., Jin, M., Zhen, B., Kong, Q. X., Song, N., ... & Si, B. Y. (2005). Study on the
885   resistance of severe acute respiratory syndrome-associated coronavirus. Journal of
886   virological methods, 126(1-2), 171-177.

887 Waterhouse, A., Bertoni, M., Bienert, S., Studer, G., Tauriello, G., Gumienny, R., Heer, F.T., de
888   Beer, T.A.P., Rempfer, C., Bordoli, L., Lepore, R., Schwede, T. SWISS-MODEL: homology
889   modelling of protein structures and complexes. Nucleic Acids Res. 46(W1), W296-W303
890   (2018).

891 Wu, F., Xiao, A., Zhang, J., Moniz, K., Endo, N., Armas, F., ... &Duvallet, C. (2020). SARS-CoV-2
892   titers in wastewater foreshadow dynamics and clinical presentation of new COVID-19
893   cases. Medrxiv.

894 Wrubleswski, J., Reichert, F. W., Galon, L., Hartmann, P. A., & Hartmann, M. T. (2018). Acute
895   and chronic toxicity of pesticides on tadpoles of Physalaemus cuvieri (Anura,
896   Leptodactylidae). Ecotoxicology, 27(3), 360-368.

897

898 Xiao, F., Sun, J., Xu, Y., Li, F., Huang, X., Li, H., ... & Zhao, J. (2020). Infectious SARS-CoV-2 in
899   feces of patient with severe COVID-19. Emerging infectious diseases, 26(8), 1920.
900 Yang, J., Wang, W., Chen, Z., Lu, S., Yang, F., Bi, Z., ... & Hong, W. (2020). A vaccine targeting
901   the RBD of the S protein of SARS-CoV-2 induces protective immunity. Nature,
902   586(7830), 572-577.
903 Yang, L., Yu, X., Wu, X., Wang, J., Yan, X., Jiang, S., & Chen, Z. (2020). Emergency response to
904   the explosive growth of health care wastes during COVID-19 pandemic in Wuhan, China.
905   Resources, Conservation and Recycling, 164, 105074.
906 Zand, A. D., & Heir, A. V. (2020). Emerging challenges in urban waste management in Tehran,
907   Iran during the COVID-19 pandemic. Resources, Conservation, and Recycling, 162,
908   105051.

909   **SUPPLEMENTARY MATERIAL**

910

911   **Table S1**. Summary information on the methodological procedures adopted in the purification stage

912   of the present study's compounds.

Compound	Retention time (min)	Purificationmethod
PSPD2001	7,7	Gradient 3 to 43% B in 90 min
PSPD2002	10,0	Gradient 10 to 50% B in 90 min
PSPD2003	2,0 e 13,3	Isocratic 2% to B in 20 min and gradient 2 to 53% B in 90 min

913   PSPD2001:   Arg-Val-Tyr-Ser-Ser-Ala-Asn-Asn-Cys-   COOH;   PSPD2002:   Gln-Cys-Val-Asn-Leu-Thr-Thr-Arg-Thr-COOH;

914   PSPD2003: Asn-Asn-Ala-Thr-Asn-COOH.

915
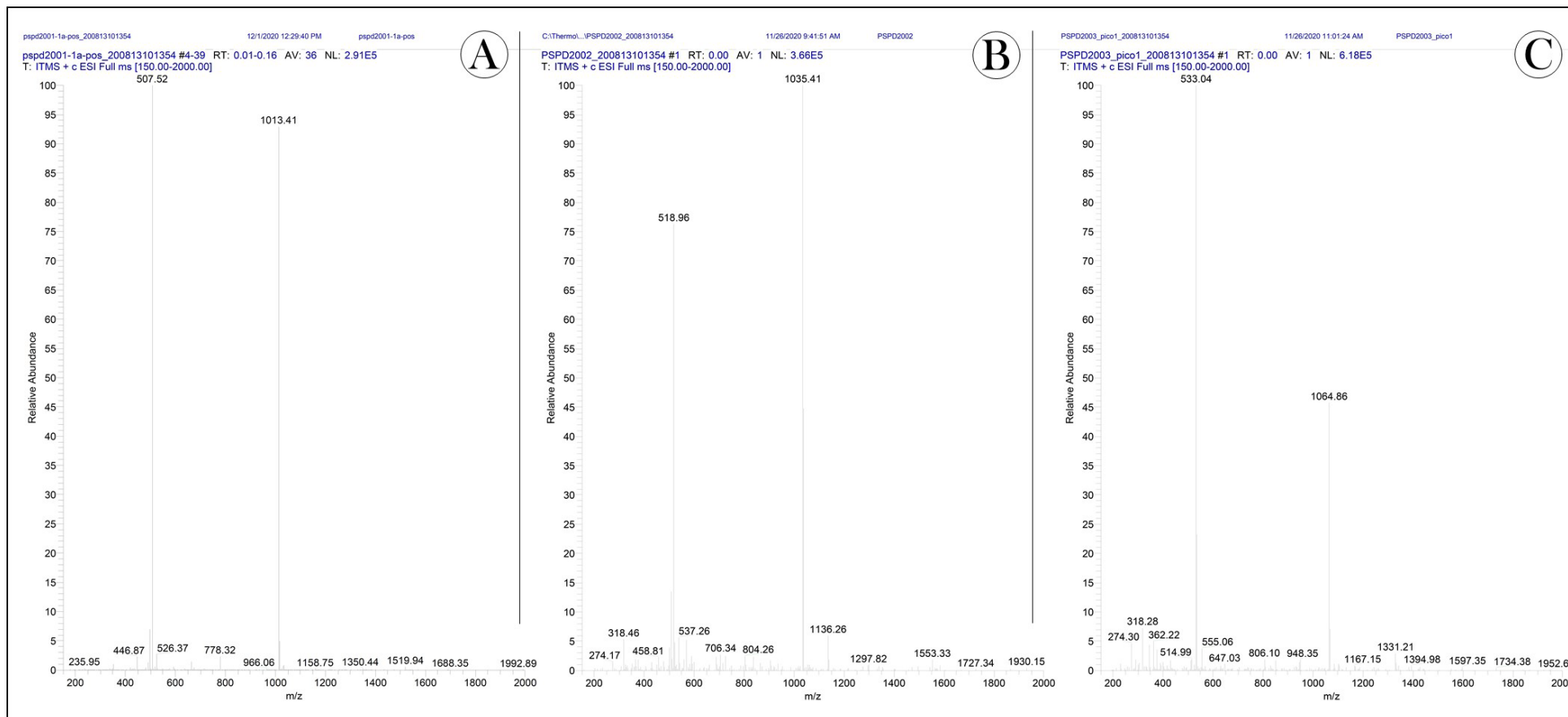
Figure S1. Mass spectra obtained for peptides (A) PSPD2001, (B) PSPD2002 and (C) PSPD2003. PSPD2001: Arg-Val-Tyr-Ser-Ser-Ala-Asn-Asn-Cys- COOH; PSPD2002: Gln-Cys-Val-Asn-Leu-Thr-Thr-Arg-Thr-COOH; PSPD2003: Asn-Asn-Ala-Thr-Asn-COOH.
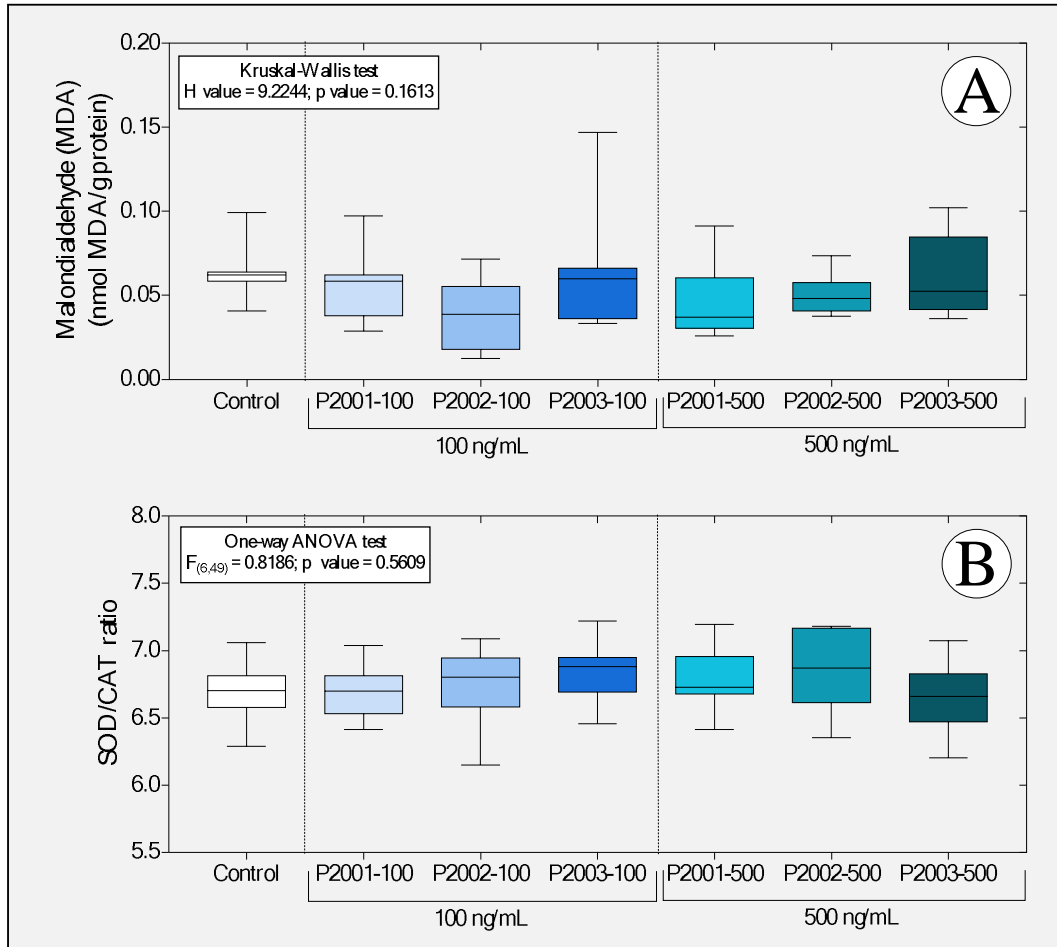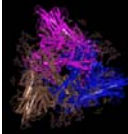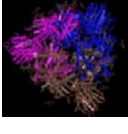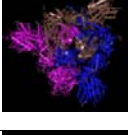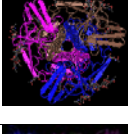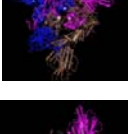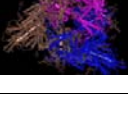
Figure S2. Boxplot of (A) concentrations of malondialdehyde and (B) SOD / CAT ratio in tadpoles of *P. cuvieri* (phase 27G) exposed or not to PSPD peptides 2001, 2002, and 2003 of the SARS-CoV-2 Spike protein. Summaries of statistical analyzes are shown in the upper left corner of the graph. (n = 50 animals / group). PSPD2001: Arg-Val-Tyr-Ser-Ser-Ala-Asn-Asn-Cys-COOH; PSPD2002: Gln-Cys-Val-Asn-Leu-Thr-Thr-Arg-Thr-COOH; PSPD2003: Asn-Asn-Ala-Thr-Asn-COOH. SOD: superoxide dismutase; CAT: catalase.

916 **TableS1:** Alignment of the sequences and consensus for PSPD2001, showing the similarities found
917 with the proteins noted in the GeneBank database by BLAST, with the Sequence ID, the protein's
918 name, the Number of Matches, the alignment and the Protein 3D Structure.

Sequence ID	Protein	Number of Matches	Alignment	Protein 3D Structure
6XR8_A	Distinct conformational states of SARS-CoV-2 spike protein [Severe acute respiratory syndrome coronavirus 2]	1	Query 1 RVYSSANNC 9 / RVYSSANNC / Sbjct 158 RVYSSANNC 166	
6XKL_A	SARS-CoV-2 HexaPro S One RBD up [Severe acute respiratory syndrome coronavirus 2]	1	Query 1 RVYSSANNC 9 / RVYSSANNC / Sbjct 158 RVYSSANNC 166	
6VSB_A	Prefusion 2019-nCoV spike glycoprotein with a single receptor-binding domain up [Severe acute respiratory syndrome coronavirus 2]	1	Query 1 RVYSSANNC 9 / RVYSSANNC / Sbjct 158 RVYSSANNC 166	
6Z43_A	Cryo-EM Structure of SARS-CoV-2 Spike : H11-D4 Nanobody Complex [Severe acute respiratory syndrome coronavirus 2]	1	Query 1 RVYSSANNC 9 / RVYSSANNC / Sbjct 158 RVYSSANNC 166	
6ZGG_A	Furin Cleaved Spike Protein of SARS-CoV-2 with One RBD Erect [Severe acute respiratory syndrome coronavirus 2]	1	Query 1 RVYSSANNC 9 / RVYSSANNC / Sbjct 189 RVYSSANNC 197	
6ZGE_A	Uncleavable Spike Protein of SARS-CoV-2 in Closed Conformation [Severe acute respiratory syndrome coronavirus 2]	1	Query 1 RVYSSANNC 9 / RVYSSANNC / Sbjct 189 RVYSSANNC 197	

919
920